TABLE II (*continued*)

T	C_{11}^{iso}	C_{11}^{ad}	C_{44}	C_{12}^{iso}	C_{12}^{ad}	B^{iso}	$\rho V_L^2[110]$	$\rho V_{T2}^2[110]$	m
				Krypton $C_{ij}(V_{T=0°K},T)$ in kbar					
5.99	48.6	48.6	24.3	23.9	24.0	32.2	60.6	12.3	12
13.30	48.1	48.6	24.1	23.7	24.2	31.9	60.5	12.2	12
59.86	46.1	51.2	22.6	23.3	28.4	30.9	62.4	11.4	12
95.82	41.8	49.3	20.0	21.9	29.5	28.5	59.4	9.92	11
99.76	45.4	54.2	21.8	23.6	32.4	30.8	65.1	10.9	12
103.5	48.9	59.1	23.7	25.2	35.3	33.1	70.9	11.9	13
				Xenon $C_{ij}(V_{expt},T)$ in kbar					
2.57	50.4		25.2	24.9		33.4	62.8	12.7	11
2.68	54.9		27.5	27.2		36.4	68.6	13.9	12
2.78	59.2		29.7	29.3		39.3	74.0	15.0	13
11.91	54.4	54.7	27.3	26.9	27.2	36.1	68.2	13.7	12
21.25	53.0	54.1	26.6	26.1	27.2	35.1	67.2	13.4	12
30.81	51.2	53.1	25.7	25.1	26.9	33.8	65.7	13.1	12
50.26	46.9	50.3	23.7	22.5	25.9	30.6	61.8	12.2	12
77.66	40.2	45.6	20.5	18.4	23.9	25.7	55.3	10.9	12
103.91	31.7	38.4	16.3	13.9	20.7	19.9	45.9	8.90	11
106.3	33.2	41.0	17.3	14.2	22.0	20.5	48.8	9.50	12
108.3	34.4	43.3	18.1	14.3	23.2	21.0	51.4	10.1	13
				Xenon $C_{ij}(V_{T=0°K},T)$ in kbar					
5.37	55.0	55.0	27.5	27.3	27.3	36.5	68.6	13.9	12
11.94	54.6	55.0	27.3	27.1	27.5	36.3	68.6	13.8	12
53.73	53.3	56.8	26.3	26.8	30.4	35.7	69.9	13.2	12
63.21	53.1	57.3	26.2	26.9	31.1	35.6	70.4	13.1	12

PHYSICAL REVIEW VOLUME 184, NUMBER 3 15 AUGUST 1969

F Center in Ionic Crystals. II. Polarizable-Ion Models

HERBERT S. BENNETT
National Bureau of Standards, Washington, D. C. 20234
(Received 26 December 1968)

The states of the *F* center are considered on the basis of models which treat the movement of the nearest neighbors to the *F* center and the *F* electron in a self-consistent manner. The lattice is first described in terms of a classical ionic-crystal theory. The theory is then extended to treat the nearest-neighbor ions in a quantum-mechanical manner. The one defect electron (the *F* electron) is treated according to polarizable-ion models. The absorption energy, the emission energy, the lifetime of the first excited state, the zero-phonon transition energies, and the Huang-Rhys factors are evaluated for two models, which differ in the rigor used to compute the polarization of the nearest and next-nearest neighbors. It is found that the model that contains the more rigorous evaluation of the polarization agrees best with the experimental results for CaO and perhaps MgO. In addition, it is found that both these models are least successful for *F* centers in NaCl and KCl. Not enough data exist to make judgments about the agreement for CaF_2, SrF_2, and BaF_2.

I. INTRODUCTION

THE *F* center in ionic crystals consists of one electron (the *F* electron) localized about a vacant anion site, regardless of the valency. Even though the *F* center is one of the simplest defects which may occur in ionic crystals, calculations of its optical properties have been a challenge to theoreticians ever since Tibbs first undertook such calculations for the alkali halides.[1] Such calculations are even today unsatisfactory in many cases when one studies the lifetimes of the excited states, the phonon structure, and the spatial extent of the *F*-electron wave function. Two basic models from which we may calculate the electronic structure of the *F* center exist. For brevity, we refer to these models as Hartree (or Hartree-Fock) polarizable-ion models (HFPI) and semicontinuum (or semicontinuum-polaron) models (SCP). Both types of models reduce a many-electron problem to an effective one-electron (the *F*-electron) problem and treat the lattice polarization and the *F* electron in a self-consistent manner. They differ most profoundly in their treatment of the effective interaction between the *F* electron and the anion vacancy due to ionic polarization. We may view the vacancy as an infinite-effective-mass hole having a charge

[1] S. R. Tibbs, Trans. Faraday Soc. **35**, 147 (1934).

$Z_v>0$. The HFPI models assume that the F-electron orbit will be small enough (or equivalently, that the F electron will move sufficiently fast) so that the ionic polarization cannot follow rapid changes in the F-electron motion. The SCP models contain an approximate expression for the F-electron-vacancy interaction which is based upon the Haken theory of Wannier excitons[2,3] and which thereby allows the ionic polarization to follow to some extent the motion of the F electron when the latter is in a large orbit (or is moving slowly).

The author has discussed, in a previous paper,[4] some of the SCP models within the context of variational procedures employing hydrogenic trial wave functions. It was found there that the SCP(HF) model was most successful for NaCl and KCl, was successful for only optical absorption in CaF_2, SrF_2, and BaF_2, and gave inconclusive results for the oxides MgO and CaO. In this paper, studies of the F center in ionic crystals are continued. Results are reported here for the F center in NaCl, KCl, MgO, CaO, SrO, CaF_2, SrF_2, and BaF_2 that follow from two HFPI models. The electronic and ionic polarizations are computed by a more rigorous procedure for the second model, HFPI (2), than for the first model, HFPI (1). Both HFPI models assert that the ionic polarization does not respond to rapid changes in the F-electron state when the F electron undergoes an optical transition. This means that all low-lying F-electron states should be compact if the model predictions are to be internally consistent with the assumptions of the model.

The method of the present calculations is a two-parameter variational procedure. The author assumes a trial wave function which has a suitable symmetry and which contains a variational parameter η. He then computes the ion displacements σ which are consistent with the assumed trial wave function. In this way, he obtains the total energy of the crystal as a function of η and σ. Finally, he minimizes the total energy as a function of η and σ to obtain the F-electron wave function and the lattice configuration.

It is found that the HFPI (1) model gives inconclusive results because the forms of the trial wave functions most likely do not approximate even crudely the exact solutions (eigenfunctions) to the HFPI (1) model. If success is measured by agreement with present experimental data, it is found that the HFPI (2) model is rather successful for CaO, is successful with some qualifications in MgO, and is least successful in the alkali halides and alkaline-earth fluorides. Making judgments about the success of a given model for the F center in the alkaline-earth fluorides is hazardous because the only known experimental data treats the absorption, and this is probably least sensitive to the physical details of a model. The above is contrasted with the SCP(HF) models of paper I. It is shown in paper I that the SCP(HF) models are successful in agreeing with the known experimental data for the alkali halides and alkaline-earth fluorides; but they give inconclusive results for the alkaline-earth oxides.

The author will review in Sec. II the classical ionic lattice and will summarize the calculation of the change in the lattice energy due to replacing an anion with an F-center electron. Using the results of Appendix A, he will list in Sec. III the many terms of the Hamiltonians for the HFPI (1) model and the HFPI (2) model. He will present in Sec. IV the theoretical expressions for those quantities which are measured in the optical absorption and emission experiments. In Sec. V, he will tabulate the numerical results of the HFPI (2) models and will discuss some additional modifications which he has studied. He will extend in Sec. VI the HFPI models to treat the nearest-neighbor ions in a quantum-mechanical manner and then will derive with reference to Appendix B the theoretical expressions for those quantities which are measured in the experiments on the zero-phonon transitions of the F center. In Sec. VII, he will compare the HFPI (2) models and the SCP(HF) models and will attempt to relate their predictions to some of the uncertainties which plague both theoretical and experimental studies. Appendix A contains a discussion of the polarizable lattice and the notation used in Sec. III. Finally, Appendix B contains the derivation of the Huang-Rhys factor for the case in which the nearest neighbors (nn) move quantum mechanically in a breathing mode and all the remaining ions move classically.

II. PRELIMINARIES

The two models for the F center which the author shall present below contain the same treatment of the lattice energy and differ only in their treatment of the contribution to the F-center energy due to the electronic and ionic polarizations. The author has given in Secs. II and III of paper I a discussion of the total crystal Hamiltonian and of the classical ionic lattice. Because he will use here the results contained in Secs. II and III of paper I, he summarizes below the contents of those two sections. He will treat first the entire lattice classically, as was done in paper I, and then in order to discuss the zero-phonon line in Sec. VI (a quantum-mechanical concept), he will treat the nn cations quantum mechanically. In this section, the entire lattice is viewed classically.

Using the Born-Oppenheimer approximation, we write the one-electron Hamiltonian for the F center as the sum of two terms,

$$\mathcal{H}_T(\mathbf{r},\mathbf{R})=\mathcal{H}_F(\mathbf{r},\mathbf{R})+\mathcal{H}_L(\mathbf{R}). \quad (1)$$

The expectation value of the operator $\mathcal{H}_F$ gives us the F-electron energy, while the expectation value of $\mathcal{H}_L$, which contains no F-electron operators, gives us the

[2] H. Haken, Nuovo Cimento **10**, 1230 (1956).
[3] H. Haken, in *Polarons and Excitons*, edited by C. G. Kuper and G. D. Whitfield (Oliver and Boyd, London, 1963), p. 295.
[4] H. S. Bennett, Phys. Rev. **169**, 730 (1968). Hereafter, we shall refer to this as paper I. We shall use, whenever possible, the notation of this reference.

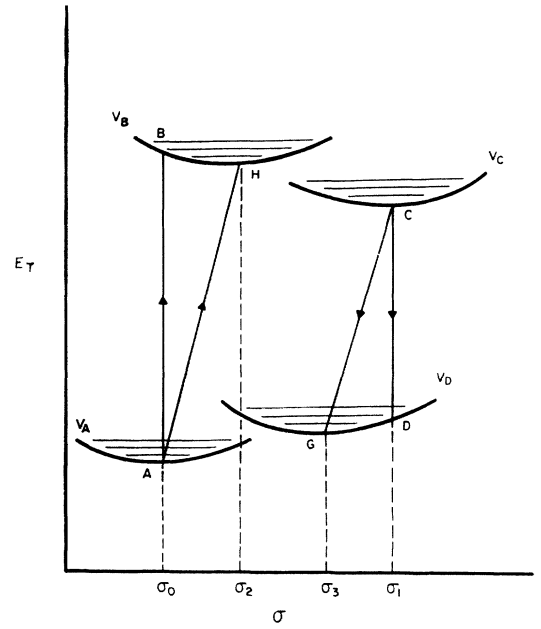

FIG. 1. Schematic configuration coordinate diagram for the HFPI (2) model in which the distant ions obey the Franck-Condon principle for all optical transitions. The quantity E_T is the total energy of the F center, and σ gives the nn radial motion $r_1'=r_1(1-\sigma)$. The points A, B, H, C, D, and G correspond, respectively, to the states $|\alpha_0;\alpha_0,\sigma_0\rangle$, $|\beta_0;\alpha_0,\sigma_0\rangle$, $|\beta_2;\alpha_0,\sigma_2\rangle$, $|\beta_1;\beta_1,\sigma_1\rangle$, $|\alpha_1;\beta_1,\sigma_1\rangle$, and $|\alpha_3;\beta_1,\sigma_3\rangle$. The F electron is in the ground state ["1s", Eq. (5)] for curves V_A and V_D, and it is in the excited state ["2p", Eq. (6)] for the curves V_B and V_C. The electronic polarization responds for all states to rapid changes in the F-electron wave function. The distant ionic polarization does not respond to the rapid changes in the F-electron wave function when it undergoes an optical transition (Franck-Condon principle). The distant ionic polarization of the lattice induced by the F electron is the same for curves V_A and V_B and is the same for curves V_C and V_D. It is computed from state $|\alpha_0;\alpha_0,\sigma_0\rangle$ for curves V_A and V_B and from state $|\beta_1;\beta_1,\sigma_1\rangle$ for curves V_C and V_D. An axis which is perpendicular to the plane of the paper and which is not drawn represents the configurations of all the distant classical ions. Curves V_A and V_B are coplanar and lie in a plane parallel to the $E_T-\sigma$ plane. Curves V_C and V_D are coplanar and lie in a plane which is parallel to the E_T-σ plane and which does not coincide with the plane in which the curves V_A and V_B lie.

lattice energy of the crystal. We shall study the following process: The F center, which is originally in its ground state $|\alpha_0;\alpha_0,\sigma_0\rangle$, becomes excited into the state $|\beta_0;\alpha_0,\sigma_0\rangle$ which is assumed to be a quasistationary state with an electronic wave function calculated from the same crystal potential (same ionic polarization) as that for the ground state $|\alpha_0;\alpha_0,\sigma_0\rangle$. We designate the total F-center state by the notation $|\eta;\zeta,\sigma\rangle$. The quantity σ gives the distance the nn ions move from their sites in a perfect lattice. The symbols η and ζ would be the generic quantum numbers in an exact description of the F center and are variational parameters in the calculations given below. The symbol α denotes a state which transforms as a "1s" state transforms, and the symbol β denotes a low-lying excited state which transforms as a "2p" state transforms. The two symbols which are to the right of the semicolon, ζ and σ, characterize the crystal potential which the F electron in the state η experiences. The lattice then relaxes and, thereby, the crystal potential which the F electron experiences changes. The excited electronic state calculated from the relaxed crystal potential $|\beta_1;\beta_1,\sigma_1\rangle$ may differ from the unrelaxed excited electronic state $|\beta_0;\alpha_0,\sigma_0\rangle$. The F center may then undergo a transition to the unrelaxed ground state $|\alpha_1;\beta_1,\sigma_1\rangle$ with an electronic wave function calculated from the same crystal potential (ionic polarization) as that for the relaxed excited state $|\beta_1;\beta_1,\sigma_1\rangle$. In Fig. 1, we present a simple configuration diagram which illustrates the four F-center states discussed above and two additional states associated with the zero-phonon transitions. We shall treat the two zero-phonon states in Sec. VI.

We want to compute the change in the lattice energy due to replacing an anion with an F-center electron. We first create a vacancy at the anion site $\mathbf{r}_0=\mathbf{0}$ of charge Z_0 by adding an effective vacancy charge $Z_v=-Z_0$ at $\mathbf{r}_0=\mathbf{0}$ and permit no lattice relaxation. This fictitious lattice state will serve as the reference energy for the lattice part of the total F-center Hamiltonian. We compute the change in the lattice energy ΔE_L (vacancy, distortion) due to replacing an anion with an F-center electron by classical ionic lattice theory. We allow the nn to move radially from r_1 to $r_1'=r_1(1-\sigma)$ in order to accommodate the F-center charge density. We define the total F-center charge density $\rho_d(\mathbf{r})$ by the relation

$$\rho_d(\mathbf{r})=\rho_F(\mathbf{r};\eta)+\rho_v(\mathbf{r}), \tag{2}$$

where the F-electron charge density is given by

$$\rho_F(\mathbf{r};\eta)=-e\psi_\eta^*(\mathbf{r})\psi_\eta(\mathbf{r}), \tag{3}$$

and where the charge density of the vacancy is given by

$$\rho_v(\mathbf{r})=Z_v\delta^3(\mathbf{r}). \tag{4}$$

The F-electron wave function is $\psi_\eta(\mathbf{r})=\langle\mathbf{r}|\eta;\zeta,\sigma\rangle_F$ and the effective vacancy charge is Z_v. The δ function $\delta^3(\mathbf{r})$ indicates that we treat the effective vacancy charge Z_v as a point charge. We also define $Z_F=-e$, where the magnitude of the electronic charge is e. The change in the lattice energy is written as the sum of many terms. Each researcher has his own way of carrying out the summations. We have chosen the method given by Eqs. (17) and (18) of paper I; i.e., the lattice energy has the form ΔE_L (vacancy, distortion) $=\Delta E_e+\Delta E_r$, where ΔE_e is the change in electrostatic energy, and ΔE_r is the change in the effective repulsive energy which takes the Pauli exclusion principle between the ith- and jth-ion cores into account. Because the van der Waal terms increase the formation energy by about 5% and decrease the distortion by about 4%, and because we do not expect the F-center-electronic part of the Hamiltonian to be accurate to within 5% of the experimental results, we do not include the van der Waal terms in our expression for the cohesive energy from

which we compute the lattice energy. In addition, because we have found previously that unless we include next-nearest-neighbor (nnn) repulsions for the oxides, the inward distortion compatible with a compact F center will be excessive, we include both first- and second-nn repulsive terms in the cohesive energy. We express the repulsive energy contribution to the cohesive energy by means of the empirically determined Born-Mayer exponential form. Again, the reader is referred to Sec. III of paper I for the details.

III. POLARIZABLE-ION MODELS

Neglecting lattice vibrations, magnetic interactions, and the spin of the F electron, we shall discuss the polarizable-ion Hamiltonian for the F center in a relaxed state ($|\alpha_0;\alpha_0,\sigma_0\rangle$ and $|\beta_1;\beta_1,\sigma_1\rangle$) and then in an unrelaxed state ($|\beta_0;\alpha_0,\sigma_0\rangle$ and $|\alpha_1;\beta_1,\sigma_1\rangle$). We mean by "relaxed" that the electronic state with a given symmetry has existed for a time long enough to allow the lattice to accommodate itself to the defect. In our case here, the F-electron state $|\eta;\eta,\sigma\rangle_F$ exists long enough for the nn ions to move. The "unrelaxed" state arises when the F-electron state $|\eta;\zeta,\sigma\rangle_F$ has existed for such a short time that the lattice has not had time to accommodate itself to the new charge density associated with the F electron. We denote the total relaxed F-center state by $|\eta;\eta,\sigma\rangle$ and the total unrelaxed F-center state by $|\eta;\zeta,\sigma\rangle$.

The trial wave functions which we shall use in the variational approach are

$$\psi_{1S}(\mathbf{r})=\langle \mathbf{r}|\alpha;\zeta,\sigma\rangle_F=(\alpha^3/7\pi)^{1/2}(1+\alpha r)e^{-\alpha r} \quad (5)$$

and

$$\psi_{2P}(\mathbf{r})=\langle \mathbf{r}|\beta;\zeta,\sigma\rangle_F=(\beta^5/\pi)^{1/2} r\cos\theta\, e^{-\beta r}, \quad (6)$$

where α and β are independent variational parameters, and ζ assumes the variational value of α for the relaxed ground state or the variational value of β for the relaxed excited state. If our calculations were exact, then the distortion σ would be the only variational parameter in the problem. The notation $|\eta;\zeta,\sigma\rangle$ means that the nn are at $r_1'=r_1(1-\sigma)$, and the ionic polarization of the remaining ions is that polarization which occurs when the F center is in the state $|\zeta;\zeta,\sigma\rangle$. The wave functions are normalized to the crystal volume

$$\int \psi_\eta^*(\mathbf{r})\psi_\eta(\mathbf{r})d^3r={}_F\langle\eta;\zeta,\sigma|\,\eta;\zeta,\sigma\rangle_F=1. \quad (7)$$

Because all terms of the model Hamiltonian operator are real, we may choose the trial wave functions $\psi_\eta(\mathbf{r})$ to be real.

Referring the reader to Appendix A for a discussion of what follows, we now list the terms of the Hamiltonians for the two polarizable-ion models. We list first those terms which are common to both model HFPI (1) and model HFPI (2).

The kinetic energy operator $\mathcal{K}_1=-(\hbar^2/2m)\nabla^2$ contributes an energy

$$H_1(\eta;\zeta,\sigma)=\int\psi^*(\mathbf{r})\mathcal{K}_1\psi(\mathbf{r})d^3r. \quad (8)$$

We consider the ions as point charges Z_ν, and we write the operator for the F-electron–point-ion interaction in the form

$$\mathcal{K}_2(\mathbf{r};\sigma)=Z_F\sum_{\nu\neq0}{}'\{Z_\nu/(\mathbf{r}-\mathbf{r}_\nu)\}, \quad (9)$$

where the prime means that the $\nu=0$ site is not included in the summation, and $\mathbf{r}_\nu$ is the location of the νth ion. The Madelung constant is defined by

$$\alpha_M=\bar{r}_1\mathcal{K}_2(0;0)/(-e), \quad (10)$$

where $\bar{r}_1$ is the nn distance (anion-cation) for the NaCl structure and is the lattice constant (cation-cation) for the CaF_2 structure. The potential energy is invariant under the full cubic group, and we may expand it in terms of the Kubic harmonics $Q(\Gamma_i,l,0)$; e.g.,

$$\mathcal{K}_2(\mathbf{r};\sigma)=V_{00}(r)Q(\Gamma_1^e,0,0;\theta\varphi)+V_{40}(r)Q(\Gamma_1^e,4,0;\theta\varphi)+\cdots+V_{n0}(r)Q(\Gamma_1^e,n,0;\theta\varphi)+\cdots,$$

where n is an even integer.[5] Because we shall limit the trial wave functions to functions which belong to the irreducible representations $\Gamma_1^e(1s)$ and $\Gamma_4^e(2p)$ of the cubic group O_h and because the following matrix elements vanish,

$$\langle\Gamma_1^e|\,Q(\Gamma_1^e,n,0;\theta\varphi|\,\Gamma_1^e\rangle=0$$

and

$$\langle\Gamma_4^e|\,Q(\Gamma_1^e,n,0;\theta,\varphi)|\,\Gamma_4^e\rangle=0,$$

for all $n\geq4$, we have that

$$\langle\eta;\zeta,\sigma|\,\mathcal{K}_2(r;\sigma)|\,\eta;\zeta,\sigma\rangle=\langle\eta;\zeta,\sigma|\,V_{\rm sph}(r;\sigma)|\,\eta;\zeta,\sigma\rangle, \quad (11)$$

where the spherically symmetric part of the point-ion-crystal potential is denoted by $V_{\rm sph}(r,\sigma)=V_{00}(r,\sigma)$.

We consider the point ions as distributed on shells centered at the anion vacancy. We denote the radius of shell s by r_s, the number of ions on shell s by S_s, and the charge of the νth ion on shell s by $Q_s=Z_\nu$. We then express the spherically symmetric part of the crystal potential $V_{\rm sph}(r,\sigma)$ in terms of the above notation, namely,

$$\begin{aligned}V_{\rm sph}(r;\sigma)&=V_0, && \text{for } 0<r<r_1'\\ &=V_0-\{(S_1Q_1/r_1')-(S_1Q_1/r_1)\}Z_\nu Z_F, && \text{for } r_1'<r<r_2\\ &=V_n+(D_n/r), && \text{for } r_n<r<r_{n+1}\end{aligned} \quad (12)$$

where

$$V_0=Z_\nu Z_F[\alpha_M/F_1+S_1Q_1\sigma/r_1(1-\sigma)],$$

[5] H. A. Bethe and F. C. Von der Lage, Phys. Rev. **71**, 612 (1947); and B. S. Gourary and F. J. Adrian, *ibid.* **105**, 1180 (1957).

where for $n \geqslant 2$ we have

$$V_n = V_0 - Z_v Z_F (S_1 Q_1/r_1' + \sum_{i=2}^{n} S_i Q_i/r_i),$$

and where

$$D_n = Z_v Z_F \sum_{i=1}^{n} S_i Q_i.$$

The term $S_1 Q_1 \sigma/r_1(1-\sigma)$ represents the total ionic polarization potential arising from the first shell owing to both the point charge Z_v and the F electron. The operator for the F-electron–point-ion interaction, $\mathcal{H}_2$, contributes the energy

$$\mathcal{H}_2(\eta;\sigma) = \int \psi^*(\mathbf{r}) V_{\text{sph}}(r,\sigma) \psi(\mathbf{r}) d^3r. \quad (13)$$

Because practical considerations limit the number of shells we may explicitly treat, we will consider the first 21 shells in our computations and will use the Coulomb potential for distances beyond the 21st shell;

$$V_{\text{sph}}(r) = Z_v Z_F/r, \quad \text{for } r > r_{21}. \quad (14)$$

We shall introduce two approximations to compute the electronic polarization and the ionic polarization induced by the defect charge density $\rho_d(\mathbf{r})$. In the first model HFPI (1), we consider only the spherically symmetric part of the polarization potential which arises from the dipoles induced on all of the ions; while in the second model HFPI (2), we consider rigorously the polarization potential from the first-two shells of dipoles ($s=1$ and $s=2$) and consider only the spherically symmetric part of the polarization potential from all the other dipoles on shells $s \geqslant 3$.

The interaction energy between the F electron and the polarization induced by the effective vacancy charge Z_v has the form

$$H_3(\eta;\sigma) = -Z_F\{Q_F(r_1';\eta) P(0; M_\nu(0,T); Z_v) + \sum_{s\geqslant 1} [Q_F(r_{s+1};\eta) - Q_F(r_s;\eta)] P(s; M_\nu(0,T), Z_v)\}. \quad (15)$$

The interaction energy between the F electron and the electronic polarization induced by the F electron has the form

$$H_{4e}(\eta\cdot\sigma) = -Z_F Z_F\{Q_F(r_1';\eta) P(0; M_\nu(0,e); Q_F(\cdots,\eta)) + \sum_{s\geqslant 1} [Q_F(r_{s+1};\eta) - Q_F(r_s;\eta)] \times P(s; M_\nu(0,e); Q_F(\cdots,\eta))\}, \quad (16)$$

and the interaction energy between the F electron in the state $|\eta;\zeta,\sigma\rangle_F$ and the ionic polarizations induced by the F electron in the state $|\zeta;\zeta,\sigma\rangle_F$ has the form

$$H_{4i}(\eta;\zeta,\sigma) = -Z_F Z_F\{Q_F(r_1';\eta) \times P(1; M_\nu(0,i); Q_F(\cdots,\zeta)) + \sum_{s\geqslant 1} [Q_F(r_{s+1};\eta) - Q_F(r_s;\eta)] \times P(s; M_\nu(0,i); Q_F(\cdots,\zeta))\}, \quad (17)$$

where $\zeta = \eta$ for the relaxed state, and ζ is the initial state of the F electron for the unrelaxed state (the final state of an optical transition). Because the HFPI models do not allow the ionic polarization to follow rapid changes in the F-electron wave function, we use the ionic polarization and the nn distortion σ which are appropriate for the initial state of an optical transition when we compute the F-electron wave function for the final state. The interaction energy $H_{4i}(\eta;\zeta,\sigma)$ then means that the F electron in the state $|\eta;\zeta,\sigma\rangle_F$ interacts with the ionic polarization potential which arises from the nn distortion σ and from the ionic dipoles induced on the distant ions in shells $s \geqslant 2$ (distant ionic polarization) by an F electron in the state $|\zeta;\zeta,\sigma\rangle_F$. We shall use hereafter this notation:

The self-energy of the F electron is[6]

$$H_{\text{se}F} = -\tfrac{1}{2}(H_{4e} + H_{4i}). \quad (18)$$

The interaction energy of Z_v with the polarization induced by Z_v itself is

$$H_5 = -Z_v P(0; M_\nu(0,T); Z_v), \quad (19)$$

and the self-energy of the effective vacancy charge is[6]

$$H_{\text{se}v} = -\tfrac{1}{2} H_5. \quad (20)$$

The interaction energy between Z_v and the electronic polarization induced by the F electron is

$$H_{6e}(\eta,\sigma) = -Z_v Z_F P(0; M_\nu(0,e); Q_F(\cdots,\eta)), \quad (21)$$

and the interaction energy between Z_v and the ionic polarization induced by the F electron is

$$H_{6i}(\zeta) = -Z_v Z_F P(1; M_\nu(0,i); Q_F(\cdots,\zeta)). \quad (22)$$

The total F-center energy for the model HFPI (1) becomes

$$H_T(\eta,\zeta,\sigma;1) = H_1 + H_2 + H_3 + \tfrac{1}{2}(H_{4e} + H_{4i}) + \tfrac{1}{2} H_5 + H_{6e} + H_{6i} + \Delta E_L(\text{vacancy, distortion}), \quad (23)$$

where $\Delta E_L(\text{vacancy, distortion}) = \Delta E_e + \Delta E_r$.

Using the notation given in Appendix A, we list the energy terms E_3 to E_{6i} for the case of model HFPI (2) which correspond to the energy terms H_3 to H_{6i} of model HFPI (1). The set of ν's corresponding to the sth shell is denoted by Γ_s.

$$E_3(\eta;\sigma) = -\{Z_v Z_F \sum_{\nu\in\Gamma_1} \alpha_1^e(Z_v) A_\nu(\eta) + Z_v Z_F \sum_{\nu\in\Gamma_2} M_-(0,T) A_\nu(\eta) + Z_F Q_F(r_3;\eta) P(3; M_\nu(0,T); Z_v) + Z_F \sum_{s\geqslant 3} [Q_F(r_{s+1};\eta) - Q_F(r_s;\eta)] P(s; M_s(0,T); Z_v)\}, \quad (24)$$

[6] T. Kojima, J. Phys. Soc. (Japan) 12, 908 (1957). Appendix A of this reference contains the derivation of Eqs. (18) and (20).

$$E_{4e}(\eta;\sigma)=-Z_F Z_F\{\sum_{\nu\in\Gamma_1}\alpha_1{}^e Q_F(\cdots,\eta)B_\nu(\eta;\eta)+\sum_{\nu\in\Gamma_2}M_-(0,e)B_\nu(\eta,\eta)+Q_F(r_3;\eta)P(3;M_\nu(0,e);Q_F(\cdots,\eta))$$
$$+\sum_{s\geqslant 3}[Q_F(r_{s+1};\eta)-Q_F(r_s;\eta)]P(s;M_s(0,e);Q_F(\cdots,\eta))\}, \quad (25)$$

$$E_{4i}(\eta;\zeta,\sigma)=-Z_F Z_F\{\sum_{\nu\in\Gamma_2}M_-(0,i)B_\nu(\eta;\zeta)+Q_F(r_3;\eta)P(3;M_\nu(0,i)Q_F(\cdots,\zeta))+\sum_{s\geqslant 3}[Q_F(r_{s+1};\eta)-Q_F(r_s;\eta)]$$
$$\times P(s;M_s(0,i);Q_F(\cdots,\zeta))\}, \quad (26)$$

$$E_{\mathrm{se}F}=-\tfrac{1}{2}(E_{4e}+E_{4i}), \quad E_5=H_5, \quad (27)$$

$$E_{\mathrm{se}v}=-\tfrac{1}{2}H_5, \quad (28)$$

$$E_{6e}(\eta,\sigma)=-Z_v Z_F\{\sum_{\nu\in\Gamma_1}\alpha_1{}^e(Q_F(\cdots,\eta))A_\nu(\eta)+\sum_{\nu\in\Gamma_2}M_-(0,e)A_\nu(\eta)+P(3;M_\nu(0,e);Q_F(\cdots,\eta))\}, \quad (29)$$

and

$$E_{6i}(\zeta)=-Z_v\{Z_F\sum_{\nu\in\Gamma_2}M_-(0,i)A_\nu(\zeta)+Z_F P(3;M_\nu(0,i);Q_F(\cdots,\zeta))\}. \quad (30)$$

The total F-center energy for the model HFPI (2) becomes

$$H_T(\eta;\zeta,\sigma;2)=H_1+H_2+E_3+\tfrac{1}{2}(E_{4e}+E_{4i})+\tfrac{1}{2}E_5$$
$$+E_{6e}+E_{6i}+\Delta E_L(\text{vacancy, distortion}). \quad (31)$$

IV. ABSORPTION AND EMISSION

The low-lying states of the F center can be described by referring to Fig. 1. The F center is originally in the relaxed ground state A, $|\alpha_0;\alpha_0,\sigma_0\rangle$. We minimize $H_T(\alpha;\alpha,\sigma\rangle$ simultaneously with respect to α and σ to obtain the energy of state A, i.e., $E_A=E_T(\alpha_0;\alpha_0,\sigma_0)$. The F center becomes excited into the state B, $|\beta_1;\alpha_0,\sigma_0\rangle$, which is assumed to be a quasistationary state with an electronic wave function calculated from the same distortion σ and distant ionic polarization as that for the relaxed ground state $|\alpha_0;\alpha_0,\sigma_0\rangle$. This is a statement of the Franck-Condon principle. It should be emphasized that the distortion σ represents the ionic displacement (ionic polarization) of the S_1 nn due to both the F electron and the effective vacancy charge Z_v, and that the distant ionic polarization (long-range ionic polarization) refers to the ionic displacements of all the remaining ions located on shells beyond the first shell. This distinction will be most important in Sec. VI when we treat the first shell of ions in a quantum mechanical manner. We minimize $H_T(\beta;\alpha_0,\sigma_0)$ with respect to only β to obtain the energy of state B, $E_B=E_T(\beta_0;\alpha_0,\sigma_0)$. The lattice then relaxes to the state C, $|\beta_1;\beta_1,\sigma_1\rangle$, and the distant ionic polarization and the nn distortion change to accommodate the F electron. We minimize $H_T(\beta;\beta,\sigma)$ simultaneously with respect to β and σ to obtain the energy of state C; i.e., $E_C=E_T(\beta_1;\beta_1,\sigma_1)$. The unrelaxed ground state D, $|\alpha_1;\beta_1,\sigma_1\rangle$, into which emission occurs is assumed to be a quasistationary state with an F-electron wave function calculated from the same distant ionic polarization and distortion σ as that for the relaxed excited state $|\beta_1;\beta_1,\sigma_1\rangle$. We minimize $H_T(\alpha;\beta_1,\sigma_1)$ with respect to only α to obtain the energy of state D, $E_D=E_T(\alpha_1;\beta_1,\sigma_1)$.[7]

The optical absorption energy for the transition from state A to state B is $E(A\text{–}B)=E_B-E_A$, and the optical emission energy from state C to state D is $E(C\text{–}D)=E_C-E_D$.

The lifetime of the relaxed excited state C is proportional to the ratio of the square of the dipole matrix elements for absorption and for emission. We expect an order-of-magnitude estimate for the radiative lifetime to be given by[8]

$$\tau=\tau_R\times 10^{-7}\ \text{sec}, \quad (32)$$

where

$$\tau_R=\frac{|\langle\beta_0;\alpha_0,\sigma_0|z|\alpha_0;\alpha_0,\sigma_0\rangle_{\mathrm{abs}}|^2}{|\langle\beta_1;\beta_1,\sigma_1|z|\alpha_1;\beta_1,\sigma_1\rangle_{\mathrm{emis}}|^2}. \quad (33)$$

We have considered only dipole radiation to the state D in the above estimate for the radiative lifetime. There are, of course, other processes which may compete with the dipole-radiation decay, such as nonradiative decay (high-temperature thermal ionization) of the excited state and tunneling to the conduction band. Hence, our present treatment of the HFPI models will be least subject to criticism for low temperatures.

The expectation value of a given power of the radial coordinate r gives us information on the spatial extent of the F-electron wave function. As a measure of the spatial extent, we have chosen to consider only the first power of r, namely,

$$r(\eta;\zeta,\sigma)=r_1{}^{-1}\langle\eta;\zeta,\sigma|r|\eta;\zeta,\sigma\rangle. \quad (34)$$

[7] The SCP(HF) and SCP(QA) models of paper I allow those ions which are sufficiently far from the F center to violate the Franck-Condon principle whenever the F-electron wave function is diffuse. Notice that in the present HFPI models the Franck-Condon principle applies to the distant ions for all F-electron wave functions. This is a most fundamental difference between the SCP models of paper I and the HFPI models of the present work.

[8] We refer the reader to Sec. V of paper I for a more complete discussion of the radiative lifetime.

TABLE I. Input data for the HFPI (1) and HFPI (2) models for the F center. The Pauling factor for the ith and the jth ions is β_{ij}. The ionic radius of the cation is ρ_+ and of the anion is ρ_-. The quantity ρ is the stiffness factor in the empirical Born-Mayer exponential form which characterizes the repulsive energy between the ith and the jth ions. The Madelung potential constant at the anion site is α_M. The high-frequency and low-frequency dielectric constants are ϵ_∞ and ϵ_0, respectively. The quantity $\bar{r}_1$ is the lattice constant (cation-cation) for the CaF_2 structure and is the nn distance (anion-cation) for the NaCl structure. The quantities β_{++}, β_{+-}, β_{--}, ϵ_∞, ϵ_0, and α_M are dimensionless. The free-ion electronic polarizabilities $\alpha_+{}^e$ and $\alpha_-{}^e$ are expressed in units of 10^{-24} cm^3. The longitudinal-optical phonon frequency ω_l is expressed in units of 10^{13} rad sec^{-1}. The letters CAW mean cation atomic weight. The CAW is used to compute the cation mass in Sec. VI. All other quantities are expressed in terms of a.u.; 1 a.u. = 27.2 eV for energy and 0.529×10^{-8} cm for length.

	NaCl	KCl	MgO	CaO	SrO	CaF_2	SrF_2	BaF_2
β_{++}	1.25	1.25	1.50	1.50	1.50	1.50	1.50	1.50
β_{+-}	1.00	1.00	1.00	1.00	1.00	1.125	1.125	1.125
β_{--}	0.75	0.75	0.50	0.50	0.50	0.75	0.75	0.75
ρ	0.599[a]	0.637[a]	0.629[b]	0.629[b]	0.629[b]	0.546[c]	0.560[c]	0.582[c]
ρ_+	2.21[a]	2.77[a]	1.76[b]	2.21[b]	2.48[b]	2.21[d]	2.48[d]	2.76[d]
ρ_-	3.00[a]	3.00[a]	2.55[b]	2.55[b]	2.55[b]	1.98[d]	1.98[d]	1.98[d]
α_M	1.748	1.748	1.748	1.748	1.748	4.071	4.071	4.071
ϵ_∞^{-1}	0.444[e]	0.469[e]	0.339[e]	0.305[e]	0.302[e]	0.489[f]	0.483[f]	0.463[f]
ϵ_0^{-1}	0.177[e]	0.214[e]	0.102[e]	0.085[e]	0.075[e]	0.149[f]	0.152[f]	0.139[f]
$\bar{r}_1$	5.31[a]	5.93[a]	3.97[b]	4.54[b]	4.86[b]	10.32[d]	10.95[d]	11.71[d]
C_4	3.579[g]	3.579[g]	3.579[g]	3.579[g]	3.579[g]	1.865[h]	1.865[h]	1.865[h]
C_6	0.9895[g]	0.9895[g]	0.9895[g]	0.9895[g]	0.9895[g]	...	...	...
C_8	2.942[g]	2.942[g]	2.942[g]	2.942[g]	2.942[g]	...	...	...
$\alpha_+{}^e$	0.41[i]	1.33[i]	0.096[j]	0.48[j]	0.86[j]	1.10[i]	1.60[i]	2.50[i]
$\alpha_-{}^e$	2.96[i]	2.96[i]	1.65[j]	2.36[j]	2.58[j]	0.64[i]	0.64[i]	0.64[i]
ω_l	4.88[e]	3.95[e]	19.83[e]	13.07[e]	8.06[e]	1.38[e]	1.12[e]	0.977[e]
CAW	22.99[k]	39.10[k]	24.32[k]	40.08[k]	87.63[k]	40.08[k]	87.63[k]	137.36[k]

[a] M. P. Tosi, in *Solid State Physics*, edited by F. Seitz and D. Turnbull (Academic Press Inc., New York, 1964), Vol. XVI, p. 52.
[b] M. L. Huggins and Y. Sakamoto, J. Phys. Soc. (Japan) **12**, 241 (1957).
[c] A. D. Franklin (private communication).
[d] G. C. Benson and E. Dempsey, Proc. Roy. Soc. (London) **A266**, 344 (1962).
[e] M. Born and K. Huang, *Dynamical Theory of Crystal Lattices* (Oxford University Press, Oxford, England, 1954), p. 85, Table 17.
[f] W. Kaiser *et al.*, Phys. Rev. **127**, 1950 (1962).
[g] A. Scholz, Phys. Status Solidi **7**, 973 (1964).
[h] H. S. Bennett, J. Res. Nat. Bur. Std. **72A**, 471 (1968).
[i] J. R. Tessman *et al.*, Phys. Rev. **92**, 890 (1953), Table VI.
[j] J. R. Tessman *et al.*, Phys. Rev. **92**, 890 (1953), Table VII.
[k] S. Glasstone, *Atomic Energy* (D. Van Nostrand Company, Inc., Princeton, N. J., 1958), p. 12.

We use the following procedure to estimate how well the variational wave functions approximate the exact eigenfunctions of our model Hamiltonians: We take the matrix elements of the operator equation

$$[z,H_T]=i\hbar p_z/m \tag{35}$$

between the states A and B for absorption and between the states C and D for emission, namely,

$$\langle\beta_0;\alpha_0,\sigma_0|z|\alpha_0;\alpha_0,\sigma_0\rangle E(A-B) = (i\hbar/m)\langle\beta_0;\alpha_0,\sigma_0|p_z|\alpha_0;\alpha_0,\sigma_0\rangle \tag{36}$$

for absorption and

$$\langle\alpha_1;\beta_1,\sigma_1|z|\beta_1;\beta_1,\sigma_1\rangle E(C-D) = (i\hbar/m)\langle\alpha_1;\beta_1,\sigma_1|p_z|\beta_1;\beta_1,\sigma_1\rangle \tag{37}$$

for emission. We then compute the left-hand and right-hand sides of Eqs. (36) and (37). If the trial wave functions $\langle\mathbf{r}|\eta;\zeta,\sigma\rangle_F$ were exact eigenfunctions of the model Hamiltonian, then the equalities of Eqs. (36) and (37) would be satisfied. However, our variational wave functions are not exact, and the amount by which the ratio $\tau_M(\zeta,\sigma)$ of the left-hand side divided by the right-hand side differs from unity will be a measure of how well we have carried out the mathematics for the HFPI models.

TABLE II. Numerical results of the HFPI (2) model for NaCl and KCl. The quantities $E(A-B)$ and $E(C-D)$ are energies expressed in atomic units (1. a.u. = 27.2 eV). All other quantities are dimensionless.

	NaCl	KCl
σ_0	0.014	0.036
$r(\alpha_0;\alpha_0,\sigma_0)$	0.725	0.703
$r(\beta_0;\alpha_0,\sigma_0)$	1.02	0.957
α_0R_0[a]	2.95	3.05
β_0R_0	2.46	2.61
$\tau_M(\alpha_0,\sigma_0)$	1.17	1.15
$E(A-B$; theory)	0.093	0.086
$E(A-B$; expt)	0.101[b]	0.085[b]
σ_1(theory)	−0.032	−0.015
σ_1(expt)	−0.07 to −0.08[c]	−0.125[c]
$r(\alpha_1;\beta_1,\sigma_1)$	0.752	0.718
$r(\beta_1;\beta_1,\sigma_1)$	1.10	0.969
α_1R_1[a]	2.85	2.98
β_1R_1	2.44	2.58
$\tau_M(\beta_1,\sigma_1)$	1.21	1.17
$E(C-D$; theory)	0.081	0.074
$E(C-D$; expt)	0.04[d]	0.046[d]
τ_R(theory)	0.86	0.87
τ_R(expt)	10.0[e]	5.71[e]

[a] The quantities R_0 and R_1 are given by the relations $R_0=r_1(1-\sigma_0)$ and $R_1=r_1(1-\sigma)_1$.
[b] J. J. Markham, in *Solid State Physics*, edited by F. Seitz and D. Turnbull (Academic Press Inc., New York, 1966), Vol. VIII (Suppl.), Table 3.2a.
[c] N. F. Mott and M. J. Littleton, Trans. Faraday Soc. **34**, 485 (1938); N. N. Kristofel', Fiz. Tverd. Tela **5**, 2367 (1963) [English transl.: Soviet Phys.—Solid State **5**, 1722 (1964)].
[d] Reference b, Table 8.1.
[e] Reference b, Table 8.5.

V. RESULTS FOR ABSORPTION AND EMISSION

In this section, the results of the preceding two HFPI models are reported. We shall divide the presentation of our results into three groups: the alkali halides (NaCl and KCl), the alkaline-earth oxides (MgO, CaO,

and SrO), and the alkaline-earth flourides (CaF_2, SrF_2, and BaF_2). We use the Born-Mayer empirical form [Eq. (15) of paper I] for the repulsive energy terms. Table I contains the values of the input data which were used in the two HFPI models.

If the test ratio τ_M is not close to unity, then we must say that our results are inconclusive because we have not solved the model Hamiltonian with sufficient rigor. We stress that even when τ_M equals unity, the variational wave functions may differ substantially from the exact wave functions. The test ratio τ_M gives us only first-moment information. The extent to which τ_M may differ from unity before we must reject the variational wave functions as being too crude for the computed quantities is a subjective decision. Our experience with the SCP models of paper I suggests that values of τ_M between 0.5 and 1.3 are reasonable.

We consider the results of the HFPI (1) model for the alkali halides, the alkaline-earth fluorides, and the alkaline-earth oxides as inconclusive because all values of the test ratio τ_M are too far from unity in both the absorption and emission studies. We may attribute this difficulty of the HFPI (1) model to the deficiencies of the hydrogenic variational wave functions. The Appendix of paper I contains a discussion of some of the deficiencies of the variational procedure. The author concludes that hydrogenic-type functions (5) and (6) do not even approximate the exact eigenfunctions of the model Hamiltonian HFPI (1).

In Table II are presented the HFPI (2) model predictions for the two alkali halides, in Table III the HFPI (2) model predictions for the three alkaline-earth oxides,

TABLE III. Numerical results of the HFPI (2) model for MgO, CaO, and SrO. The quantities $E(A-B)$ and $E(C-D)$ are energies expressed in a.u. (1 a.u.=27.2 eV). All other quantities are dimensionless.

	MgO	CaO	SrO
σ_0	−0.067	−0.055	−0.048
$r(\alpha_0;\alpha_0,\sigma_0)$	0.709	0.673	0.658
$r(\beta_0;\alpha_0,\sigma_0)$	1.04	0.947	0.906
$\alpha_0 R_0$ [a]	3.02	3.18	3.26
$\beta_0 R_0$	2.41	2.64	2.76
$\tau_M(\alpha_0,\sigma_0)$	1.28	1.23	1.21
$E(A-B$; theory)	0.141	0.127	0.120
$E(A-B$; expt)	0.180[b]; 0.182[c]	0.134[c]	0.110[b]; 0.118±0.02[d]
σ_1	−0.090	−0.074	−0.066
$r(\alpha_1;\beta_1,\sigma_1)$	0.751	0.700	0.678
$r(\beta_1;\beta_1,\sigma_1)$	1.06	0.944	0.905
$\alpha_1 R_1$ [a]	2.85	3.06	3.17
$\beta_1 R_1$	2.37	2.65	2.76
$\tau_M(\beta_1,\sigma_1)$	1.37	1.27	1.23
$E(C-D$; theory)	0.127	0.119	0.113
$E(C-D$; expt)	0.088[e]	0.121[e]	0.090±0.01[d]
τ_R(theory)	0.86	0.90	0.92

[a] The quantities R_0 and R_1 are given by the relations $R_0=r_1(1-\sigma_0)$ and $R_1=r_1(1-\sigma_1)$.
[b] B. Henderson *et al.*, J. Phys. **C1**, 586 (1968), Table 2; and B. Henderson, Natl. Bur. Std. (U. S.) Spec. Publ. **296**, 41 (1967).
[c] J. C. Kemp *et al.*, Phys. Rev. **171**, 1024 (1968); and B. D. Evans *et al.*, Phys. Letters **27A**, 506 (1968).
[d] B. D. Evans (private communications). These are preliminary and unpublished results for which the author thanks B. D. Evans.
[e] Ref. b. Because the Huang-Rhys factor is experimentally about 39, the F-center emission peak has not been observed in MgO. The authors estimate that it is near 0.088 a.u.

TABLE. IV. Numerical results of the HFPI (2) model for CaF_2, SrF_2, and BaF_2. The quantities $E(A-B)$ and $E(C-D)$ are energies expressed in a.u. (1 a.u.=27.2 eV). All other quantities are dimensionless.

	CaF_2	SrF_2	BaF_2
σ_0	0.042	0.041	0.041
$r(\alpha_0;\alpha_0,\sigma_0)$	0.732	0.721	0.709
$r(\beta_0;\alpha_0,\sigma_0)$	0.993	0.972	0.947
$\alpha_0 R_0$ [a]	2.93	2.97	3.02
$\beta_0 R_0$	2.52	2.57	2.64
$\tau_M(\alpha_0,\sigma_0)$	1.16	1.16	1.15
$E(A-B$; theory)	0.142	0.131	0.119
$E(A-B$; expt)	0.121[b]	0.101[b]	0.069[b]
σ_1	−0.004	−0.005	−0.006
$r(\alpha_1;\beta_1,\sigma_1)$	0.754	0.740	0.725
$r(\beta_1;\beta_1,\sigma_1)$	1.02	1.00	0.974
$\alpha_1 R_1$ [a]	2.84	2.89	2.85
$\beta_1 R_1$	2.45	2.50	2.57
$\tau_M(\beta_1,\sigma_1)$	1.20	1.19	1.18
$E(C-D$; theory)	0.125	0.115	0.105
$E(C-D$; expt) [c]	...	...	...
τ_R(theory)	0.86	0.86	0.87

[a] The quantities R_0 and R_1 are given by the relations $R_0=r_1(1-\sigma_0)$ and $R_1=r_1(1-\sigma_1)$.
[b] P. Feltham and I. Anders, Phys. Status Solidi **10**, 203 (1965), Table 3.
[c] Experimental values for emission have not been reported.

and in Table IV the HFPI (2) model predictions for the three alkaline-earth fluorides.

Two modifications to the HFPI (1) and HFPI (2) models have also been studied. The first modification contains a different evaluation of the electronic polarization. Namely, during an optical transition the electronic polarization induced by the F electron responds to only the change in the F-electron charge density of each state. These modifications are called the HFPI (1, mod) and HFPI (2, mod) models. The absorption problem may be used as an example in order to be more explicit. The electronic polarization induced by the F electron for the state $B\equiv|\beta_0;\alpha_0,\sigma_0\rangle$ may be obtained from the electron polarization induced by the F electron for the state $A\equiv|\alpha_0;\alpha_0,\sigma_0\rangle$ by adding the electronic polarization induced by the change in the charge density between the final and the initial states $Q_F(r;\beta_0;\alpha_0,\sigma_0)-Q_F(r;\alpha_0;\alpha_0,\sigma_0)$. For all the quantities given in Tables II, III, and IV, there are only negligible differences between the HFPI (1, mod) model and the HFPI (1) model and between the HFPI (2, mod) model and the HFPI (2) model. Also, the analogs of Eqs. (15)–(31) are much lengthier than any of those equations. Therefore, we do not report the numerical results for these models. The HFPI (1, mod) model yields test ratios τ_M which are much too large and the HFPI (2, mod) model agrees with the HFPI (2) model to within 3%. The latter result obtains because all states are rather compact.

The second modification attempts to study the finite-ion-size effect and approximates the Coulomb-interaction integrals between the F electron and the first- and second-nn core electrons. This second modification neglects the exchange integrals and hence is subject to question. We mention the second modification here only

because we want to avoid confusing its results with the present results. We replace in the second modification[9] the point charges of the first- and second-nn by spherically symmetric charge densities of the form $C_\nu(r)=(a_\nu e^{-b_\nu r})^2$, where r is the radial distance from the νth ion on shells $s=1$ and $s=2$. The conditions

$$4\pi\int_0^\infty C_\nu(r)r^2dr=Z_\nu$$

and

$$4\pi\int_0^{\rho_\nu} C_\nu(r)r^2dr=0.9Z_\nu$$

determine the parameters a_ν and b_ν for the νth ion. The second condition states that 90% of the ionic charge is contained within a sphere whose radius is the ionic radius, $\rho_\nu=\rho_+$ for cations, and $\rho_\nu=\rho_-$ for anions. We evaluate the Coulomb integrals between this effective ionic charge density and the F-electron wave function and thereby obtain, in a most heuristic manner, the effect of the finite size of the nn and nnn ions on the self-consistent potential which the F electron experiences. We then proceed as in the HFPI (1) model and call this second modification the HFPI (1, finite-ion) model. Using this model, we studied the F center in CaO and reported the results in Ref. 9. Except for the absorption energy, only a negligible numerical difference exists between the HFPI (2) model and the HFPI (1, finite-ion) model. The HFPI (2) model predicts $E(A-B)=0.127$ a.u. and the HFPI (1, finite-ion) model predicts $E(A-B)=0.133$ a.u. We feel that any model such as the HFPI (1, finite-ion) model which approximates the Coulomb interaction integrals between the F electron and the core electrons should include also an evaluation of the exchange-interaction integrals to determine their values relative to the Coulomb-interaction integrals. We expect that this second modification is justified only for very compact F-electron states, $r(\eta;\zeta,\sigma)\lesssim 0.6$, and for very compact core-electron states. This is the case for which the F-electron–core-electron overlap integrals are small and for which exchange integrals may be neglected. We doubt that all the F-electron and core-electron states meet these conditions, and for this reason, we shall not discuss the HFPI (1, finite-ion) model any further.

VI. QUANTUM LATTICE

The F-center absorption and emission in CaO exhibit some structure which Henderson[10] and Kemp[11] interpret to be zero-phonon lines. The concept of zero-phonon lines is a quantum-mechanical concept. In this section, we shall extend our models to treat the nn ions in a quantum-mechanical manner. We shall continue to treat classically the ions on shells $s\geq 2$. The quantum-mechanical model which we present is very idealized. We assume that the nn ions are constrained to move only in the breathing mode.

We write the total idealized F-center Hamiltonian as

$$\mathcal{H}_T=T_F+T_N+V(r,X)+V_i(r;\zeta)+V_e(r;\eta)+\tfrac{1}{2}\mathcal{H}_5 +\Delta E_L(\text{vacancy, distortion}). \quad (38)$$

Here T_F is the F-electron kinetic energy; T_N is the kinetic energy of the S_1 nn ions; and X represents the positions of the S_1 nn, i.e., $\mathbf{X}_\nu=\mathbf{r}_\nu(1-\sigma)$ for the breathing mode. We now treat, in the Hamiltonian of Eq. (38) the F electron and the S_1 neighbors in a quantum-mechanical manner and all the remaining ions in a classical manner. We shall define below the potential operators V, V_i, V_e, and $\mathcal{H}_5$.

The Born-Oppenheimer approximation separates the total wave function $\Psi_{\eta,n}$ into electronic and nuclear factors:

$$\Psi_{\eta,n}=\psi_\eta(r;X)\chi_{\eta,n}(X), \quad (39)$$

where the F-electron wave function $\langle r\,|\,\eta;\zeta,\sigma\rangle_F=\psi_\eta(r;X)$ depends parametrically on the ion (nuclear) coordinate, and where the ion (nuclear) wave function $\langle X\,|\,\eta;\zeta,\sigma\rangle=\chi_{\eta,n}(X)$ depends not on the F-electron coordinate r but on the F-electron state η. We define, within the context of the Born-Oppenheimer approximation, the potential operators V, V_i, V_e, and $\mathcal{H}_5$ by the identifications

$$\langle\eta;\zeta,\sigma\,|\,V(r,X)\,|\,\eta;\zeta,\sigma\rangle=H_2(\eta;\sigma)+E_3(\eta;\sigma), \quad (40)$$

$$\langle\eta;\zeta,\sigma\,|\,V_i(r,\zeta)\,|\,\eta;\zeta,\sigma\rangle=E_{6i}(\zeta)+\tfrac{1}{2}E_{4i}(\eta;\zeta,\sigma), \quad (41)$$

$$\langle\eta;\zeta,\sigma\,|\,V_e(r,\eta)\,|\,\eta;\zeta,\sigma\rangle=E_{6e}(\eta,\sigma)+\tfrac{1}{2}E_{4e}(\eta;\sigma), \quad (42)$$

$$\langle\eta;\zeta,\sigma\,|\,\mathcal{H}_5\,|\,\eta;\zeta,\sigma\rangle=H_5, \quad (43)$$

and the F-electron kinetic-energy operator by the identification

$$\langle\eta;\zeta,\sigma\,|\,T_F\,|\,\eta;\zeta,\sigma\rangle=H_1(\eta;\sigma). \quad (44)$$

Using the Born-Oppenheimer approximation, we obtain the following equations for the F-electron and nuclear systems:

$$\{T_e+V(r;X)+V_i(r;\zeta)+V_e(r;\eta)\}\psi_\eta(r;X) =H_F(\eta;\zeta,\sigma)\psi_\eta(r,X), \quad (45)$$

and

$$\{T_N+H_F(\eta;\zeta,\sigma)+\Delta E_L(\sigma)\}\chi_{\eta,n}(X)=\mathcal{E}_{n,\eta}\chi_{\eta,n}(X), \quad (46)$$

where

$$T_N=-\frac{\hbar^2}{2M}\sum_{\nu\in\Gamma_1}^{S_1}\nabla_\nu^2;$$

M is the mass of the ion at $\mathbf{r}_\nu$ on the first shell,

$$\nabla_\nu=\hat{x}\frac{\partial}{\partial X_{\nu,x}}+\hat{y}\frac{\partial}{\partial X_{\nu,y}}+\hat{z}\frac{\partial}{\partial X_{\nu,z}},$$

$$\Delta E_L(\sigma)=\Delta E_L(\text{vacancy, distortion})+\tfrac{1}{2}H_5,$$

[9] H. S. Bennett, Bull. Am. Phys. Soc. **13**, 420 (1968).
[10] B. Henderson, Natl. Bur. Std. (U. S.) Spec. Publ. **296**, 41 (1968).
[11] J. C. Kemp *et al.*, Phys. Rev. **171**, 1024 (1968).

and

$$H_F(\eta;\zeta,\sigma)=H_T(\eta;\zeta,\sigma)-\Delta E_L(\sigma).$$

In order to proceed further, we introduce the harmonic approximation. The total energy $H_T(\eta;\zeta,\sigma)$ has a minimum at $\sigma_m(\eta;\zeta)$. For example, our results in Sec. V tell us that $\sigma_m(\alpha_0;\alpha_0)=\sigma_0$ and $\sigma_m(\beta_1;\beta_1)=\sigma_1$. We expand the total energy about the minimum σ_m to second order; i.e.,

$$H_T(\eta;\zeta,\sigma)\approx H_T(\eta;\zeta,\sigma_m)+\tfrac{1}{2}S_1M\omega_m^2(\eta;\zeta)r_1^2(\sigma-\sigma_m)^2, \quad (47)$$

where the relation

$$S_1M\omega_m^2(\eta;\zeta)=r_1^{-2}\left.\frac{\partial^2H_T(\eta;\zeta,\sigma)}{\partial\sigma^2}\right|_{\sigma=\sigma_m} \quad (48)$$

defines the local breathing-mode frequency $\omega_m(\eta;\zeta)$ and r_1 is the nn distance for the perfect lattice. The lattice equation (46) becomes

$$\sum_{\nu\in\Gamma_1}^{S_1}\left\{-\frac{\hbar^2}{2Mr_1^2}\frac{\partial^2}{\partial\sigma^2}+\tfrac{1}{2}[M\omega_m^2(\eta;\zeta)r_1^2(\sigma-\sigma_m)^2]\right\}\chi_{\eta,n}(X)=\{\mathcal{E}_{n,\eta}-H_T(\eta;\zeta,\sigma_m)\}\chi_{\eta,n}(X). \quad (49)$$

Equation (49) is separable, and we therefore write the breathing-mode–lattice wave function as the product wave function

$$\chi_{\eta,n}(X)=\prod_{\nu\in\Gamma_1}^{S_1}U_{\eta,n}(X_\nu), \quad (50)$$

where $U_{\eta,m}(X_\nu)=U_{\eta,n}(X_\nu')$ for all ν and ν' on the first shell. The individual-ion wave functions satisfy the equation

$$\sum_{\nu\in\Gamma_1}^{S_1}-\frac{\hbar^2}{2Mr_1^2U_{\eta,n}(X_\nu)}\frac{\partial^2U_{\eta,n}(X_\nu)}{\partial\sigma^2}+\tfrac{1}{2}M\omega_m^2(\eta;\zeta)r_1^2(\sigma-\sigma_m)^2=\mathcal{E}_{n,\eta}-H_T(\eta;\zeta,\sigma_m). \quad (51)$$

We see from Eq. (51) that the quantum-mechanical lattice reduces within the context of the Born-Oppenheimer and the harmonic-lattice approximations to the solution of the Schrödinger equation for the harmonic oscillator. Letting $y_m=r_1(\sigma-\sigma_m)$, we have finally

$$\left\{-\frac{\hbar^2}{2M}\frac{\partial^2}{\partial y_m^2}+\tfrac{1}{2}M\omega_m^2(\eta;\zeta)y_m^2\right\}U_{\eta,n}(y_m)=S_1^{-1}\{\mathcal{E}_{n,\eta}-H_T(\eta;\zeta,\sigma_m)\}U_{n,\eta}(y_m). \quad (52)$$

Hence, the eigenvalue for each ion is

$$S_1^{-1}\{\mathcal{E}_{n,\eta}-H_T(\eta;\zeta,\sigma_m)\}=\hbar\omega_m(\eta;\zeta)(n+\tfrac{1}{2}), \quad (53)$$

and the wave function for each ion is

$$U_{\eta,n}(y_m)=N_nH_n(\gamma_my_m)e^{-\frac{1}{2}\gamma_m^2y_m^2}, \quad (54)$$

where $n=0, 1, 2, 3,\cdots$,

$$N_n=(\gamma_m/\sqrt{\pi}\,2^nn!)^{1/2}, \quad \gamma_m^2=(M\omega_m/\hbar),$$

$H_n(\xi)$ is the Hermite polynomial of order n, e.g., $H_0(\xi)=1$, $H_1(\xi)=2\xi$, etc., and where $\xi=\gamma_my_m$.

When we treat the breathing mode of the first S_1 nn quantum mechanically, the total F-center energy becomes

$$E_{TQ}=\mathcal{E}_{n,\eta}=H_T(\eta;\zeta,\sigma_m)+\hbar\omega_m(n+\tfrac{1}{2}). \quad (55)$$

We see from Eq. (55) that the total energy E_{TQ} should be minimized to obtain the correct F-center energy. That is, we should find the appropriate minimum of $H_T(\eta;\zeta,\sigma_m)$, e.g., $E_T(\eta_t;\zeta_t,\sigma_t)$, use this energy to compute the frequency ω_t, and calculate the total quantum energy E_{TQ}. We then should vary, simultaneously, the parameters η, ζ, and σ about the respective values η_t, ζ_t, and σ_t, compute a new $\omega_t(\eta;\zeta,\sigma)$, and thereby, a new E_{TQ}. These steps should be repeated until the minimum of E_{TQ} obtains. But this iteration procedure requires excessive computer time. We, therefore, use below the results from the first step of the above iteration procedure. We expect the error to be negligible because $m\ll M$ and therefore $\langle T_e\rangle\gg\langle T_N\rangle$.

At this point in our discussion, let us consider how we calculate the states G and H of Fig. 1 and how we evaluate the local frequencies $\omega_m(\eta;\zeta,\sigma_m)$. We minimize $H_T(\beta;\alpha_0,\sigma)$ simultaneously with respect to β and σ to obtain the energy of state H, i.e., $E_H=E_T(\beta_2;\alpha_0,\sigma_2)$. This notation means that the distant ionic polarization for state H is the same as that for states A and B. Similarly, we minimize $H_T(\alpha;\beta_1,\sigma)$ simultaneously with respect to α and σ to obtain the energy of state G, i.e., $E_G=E_T(\alpha_3;\mathcal{E}_1,\sigma_3)$. This notation means that the distant ionic polarization for state G is the same as that for states C and D. Let us summarize the polarizations in the six F-center states. The electronic polarization is different for all six states A, B, H, C, D, and G. The distant ionic polarization ($s\gtrsim 2$) is the same for states A, B, and H and for the states C, D, and G; but that for states C, D, and G differs from that for states A, B, and H. States A and B have the same distortion σ_0, and states C and D have the same distortion $\sigma_1\neq\sigma_0$.

We compute the local breathing-mode frequencies from the following relations:

$$\omega_0^2(\alpha_0;\sigma_0)=\frac{2\{E_A(0.01)-E_A\}}{S_1Mr_1^2(0.01)^2}, \quad (56)$$

$$\omega_1^2(\beta_1;\sigma_1)=\frac{2\{E_C(0.01)-E_C\}}{S_1Mr_1^2(0.01)^2}, \quad (57)$$

$$\omega_2^2(\alpha_0;\sigma_2)=\frac{2\{E_B-E_H\}}{S_1Mr_1^2(\sigma_2-\sigma_0)^2}, \quad (58)$$

$$\omega_3^2(\beta_1;\sigma_3)=\frac{2(E_D-E_G)}{S_1Mr_1^2(\sigma_3-\sigma_1)^2}, \quad (59)$$

TABLE V. Numerical results of the HFPI (2) model for the zero-phonon transitions. The quantities E(0-ph) are energies expressed in a.u. (1 a.u. = 27.2 eV). All other quantities are dimensionless.

	NaCl	KCl	MgO	CaO	SrO	CaF_2	SrF_2	BaF_2
S(abs; theory)	7.81	11.39	3.56	3.56	4.43	7.53	11.07	14.19
S(abs; expt)	25.0[a]	...	39.0[b]	3.9[c]	...	...	...	...
E(0-ph; abs,theory)	0.085	0.079	0.132	0.122	0.116	0.132	0.122	0.111
E(0-ph; abs,expt)	...	...	0.134[b]	0.128[c]	...	...	...	...
n_B	7.33	11.05	3.00	3.04	3.95	7.27	10.87	14.14
S(emis; theory)	6.15	10.05	2.61	2.46	3.26	7.48	11.04	14.50
S(emis; expt)	...	...	...	3.5 to 4.9[c]	...	...	...	...
E(0-ph; emis,theory)	0.086	0.079	0.134	0.123	0.117	0.134	0.123	0.112
E(0-ph; emis,expt)	...	...	0.134[b]	0.128[c]	...	...	...	...
n_D	5.57	9.27	2.22	1.98	2.78	6.77	10.34	13.65

[a] J. J. Markham, in *Solid State Physics*, edited by F. Seitz and D. Turnbull (Academic Press Inc., New York, 1966), Vol. VIII, (Suppl.), Table 3.5. The Huang-Rhys factor is assumed to be 25 for the Poissonian curve.
[b] B. Henderson *et al.*, J. Phys. C (Proc. Phys. Soc.), **1**, 586 (1968), Table 2; and B. Henderson, Natl. Bur. Std. (U. S.), Spec. Publ. **296**, 41 (1967). These values are estimates.
[c] J. C. Kemp *et al.*, Phys. Rev. **171**, 1024 (1968); and B. D. Evans, Phys. Letters **27A**, 506 (1968).

where we minimize $H_T(\alpha;\alpha_0,\sigma_0-0.01)$ with respect to α only to obtain the energy

$$E_A(0.01)=E_T(\alpha';\alpha_0,\sigma_0-0.01)$$

and $H_T(\beta;\beta_1,\sigma_1-0.01)$ with respect to β only to obtain the energy $E_C(0.01)=E_T(\beta';\beta_1,\sigma_1-0.01)$.

When the quantum number n is large, we define the classical turning point as that displacement $\sigma_{c1}(n,m)$ for which the kinetic energy of the oscillating ion is zero, namely,

$$\tfrac{1}{2}M\omega_m^2r_1^2[\sigma_{c1}(n,m)-\sigma_m]^2=\hbar\omega_m(n+\tfrac{1}{2}). \quad (60)$$

The oscillator quantum number is zero for the states A, C, G, and H, and it is approximately

$$n_B=[M\omega_2^2r_1^2(\sigma_0-\sigma_2)^2-\hbar\omega_2]/2\hbar\omega_2 \quad (61)$$

for state B and

$$n_D=[M\omega_3^2r_1^2(\sigma_1-\sigma_3)^2-\hbar\omega_3]/2\hbar\omega_3, \quad (62)$$

for state D.

Before we calculate the zero-phonon transition energy in terms of the above quantum lattice, we must emphasize the difference between the experimental F center examined in the laboratory and the idealized F center described by Eqs. (38) and (39). The experimental F center is a complete quantum system for all ions ($s=1$ and $s\geqslant 2$) and for the defect electron. It does not have any obligation to satisfy the Born-Oppenheimer approximation and the Franck-Condon principle. The final state of a zero-phonon transition which occurs in the laboratory is a totally relaxed state. Because the experimental F center emits no additional phonons after a zero-phonon transition, the distant ions, which behave quantum mechanically, also relax during the optical transition. Unfortunately, because we are forced for practical reasons to treat the distant ions classically and the nn ions quantum mechanically, we destroy our ability to describe the zero-phonon transition in an entirely satisfactory manner. Given the HFPI model, we must calculate correctly within its framework the zero-phonon transitions. The idealized F center (the HFPI model considered here) satisfies the Born-Oppenheimer approximation for all states. Because the distant ions have behave classically in the HFPI model, they exhibit no zero-point motion and hence must satisfy the Franck-Condon principle during any optical transition. Also, as a result of this classical treatment of the distant ions, the HFPI model contains no direct mechanism for relaxing the distant ions during an optical transition. That is to say, the probability that the distant ions are at positions other than their positions appropriate for the relaxed state A for absorption or the relaxed state C for emission is zero. This is not the case for the nn ions. Their quantum behavior gives them a finite (nonzero) probability to be at positions other than σ_0(absorption) or σ_1(emission). This classical aspect of the model introduces a surprising behavior in view of present thought when we treat the zero-phonon transition within the restraints of the Born-Oppenheimer approximation and the Franck-Condon principle for the distant ions. The model allows the zero-phonon transition energy and the Huang-Rhys factor in absorption to differ from the corresponding quantities in emission [Eqs. (63)–(66)]. Experimental data on the zero-phonon transitions for F centers are scarce. The present interpretations of the experimental data suggest that E(0-ph; abs,expt) equals to within experimental error E(0-ph; emis,expt) and that S(abs; expt), the absorption Huang-Rhys factor, differs from S(emis; expt), the emission Huang-Rhys factor. We refer the reader to Table V. This subtle theoretical and model-dependent feature may be of no quantitative consequence when we insert numbers into the model. In fact, we shall show for the crystals studied here that this is the case.

The above discussion suggests that we should consider modifying the model to treat the zero-phonon transitions in a more realistic manner. However, any practical modification would destroy the internal consistency of the present model for some of the states and would add more unknown parameters. These additional parameters would be associated with the coupling between the immediate neighbors to the defect and the distant ions.

We choose instead to calculate within the context of the HFPI (2) model the zero-phonon transition energies and the Huang-Rhys factors and then to see what it then predicts numerically. We shall find that E(0-ph; abs,theory)$\approx E$(0-ph; emis,theory) to within 2%. Hence the model does agree with present experiments on the near equality of E(0-ph; abs) and E(0-ph; emis).

Other researchers might prefer altering the model in order to treat more realistically the zero-phonon transitions. But unless their resulting model is completely quantum mechanical and treats all ions in the same manner, they also will be forced by practical considerations to choose between equally and physically unsatisfactory alternatives and to add additional parameters. For example, consider the model in which the F center consists of the one-defect electron and only the S_1-nn ions. The one-electron and S_1 ions all behave quantum mechanically. We neglect completely the distant ions ($s\geqslant 2$). Let us call this greatly reduced model the HFPI [nn only, quantum-mechanical (QM)] model. The configuration diagram for the HFPI (nn only, QM) model which corresponds to Fig. 1 for the HFPI (2) model appears similar to Fig. 1 in paper I. Referring to Fig. 1 in the present paper, we find that the curves V_A and V_D coincide, the curves V_B and V_C coincide, the points A and G coincide, and the points C and H coincide. In addition, the resulting curves $V_A(V_D)$ and $V_C(V_B)$ both lie in the E_T-σ plane. The zero-phonon transition for the HFPI (nn only, QM) model is between states A and C. However, even though we may calculate now the zero-phonon transition correctly and without any ambiguities, the HFPI (nn only, QM) model is not physically satisfactory for the optical transitions from A to B or from C to D. These transitions are greatly influenced by the more distant ions which are neglected in the HFPI (nn only, QM) model.

Such problems associated with the distant ions plague all theoretical treatments. Also, the theories on the zero-phonon transition depend upon the validity of the Born-Oppenheimer approximation. The concepts by which researchers attempt to overcome the distant-ion problem are one of the main features which distinguish the many models for the F center from one another. We shall return to this in Sec. VII.

A zero-phonon transition occurs within the limited context of the idealized quantum lattice of model HFPI whenever the quantum number n does not change during the transition, and whenever the distant ions ($s\geqslant 2$) do not move in accordance with the Franck-Condon principle. A finite probability that the nn ions for state A may be at σ_2 instead of at σ_0 exists because of the zero-point motion. If during an optical transition from state A(or C), the nn ions (quantum) move to σ_2(or to σ_3) because of their zero-point motion, then a zero-phonon transition is possible. Hence, the existence of zero-phonon transitions for the HFPI models means that the nn ions (quantum) may violate the Franck-Condon principle, but that the distant ions (classical) ($s\geqslant 2$) must satisfy the Franck-Condon principle. The transitions from states A to H and from states C to G correspond, respectively, to the idealized zero-phonon transition in absorption and to the idealized zero-phonon transition in emission. The optical energy for the idealized zero-phonon transition in absorption is

$$E(\text{0-ph; abs,theory})=E_H-E_A\,, \tag{63}$$

and that in emission is

$$E(\text{0-ph; emis,theory})=E_C-E_G\,. \tag{64}$$

The probability for the zero-phonon-absorption transition from state A, with $n_A=0$, to the state H, with $n_H=0$, relative to the entire F-center absorption band is $e^{-S_{\text{abs}}}$, where S_{abs} is the absorption Huang-Rhys factor Similarly, the probability for the zero-phonon-emission transition from state C, with $n_C=0$, to state G, with $n_G=0$, relative to the entire F-center emission band is $e^{-S_{\text{emis}}}$, where S_{emis} is the emission Huang-Rhys factor. We derive in Appendix B the expressions for S_{abs} and for S_{emis}. From Eq. (B11) we have that

$$S_{\text{abs}}=S_1\gamma_0{}^2r_1{}^2(\sigma_2-\sigma_0)^2/(1+\gamma_{\text{abs}}{}^2) \tag{65}$$

and

$$S_{\text{emis}}=S_1\gamma_1{}^2r_1{}^2(\sigma_3-\sigma_1)^2/(1+\gamma_{\text{emi}},{}^2)\,, \tag{66}$$

where $\gamma_{\text{abs}}=\gamma_0/\gamma_2$ and $\gamma_{\text{emis}}=\gamma_1/\gamma_3$.

We list in Table V the oscillator quantum numbers n_B and n_D, the idealized-zero-phonon transition energies, and the Huang-Rhys factors for the HFPI (2) model and compare them with their experimental values. We observe that

$$E(\text{0-ph; abs,theory})\approx E(\text{0-ph; emis,theory})\,.$$

This agrees with the limited number of experiments reported.

VII. COMMENTS AND DISCUSSION

The author uses in both the SCP models of paper I and the present HFPI models a variational procedure with trial F-electron wave functions to approximate the exact solutions to model Hamiltonians. The variational ground-state energy is known to be greater than the exact ground-state eigenvalue. But, it is not known whether an excited-state energy will be greater than or less than the exact excited-state eigenvalue. The test ratios $\tau_M(\zeta,\sigma)$ indicate to what extent the trial wave functions approximate the exact solutions of the model Hamiltonians. Another feature which is common to both the SCP and HFPI models is the implicit assumption that radial changes in the F-electron wave function dominate in determining the energy levels and the lifetimes of excited states. Recent experimental data[12] and preliminary theoretical studies[13] suggest that radial and angular changes may be both equally important.

[12] L. D. Bogan, thesis, Cornell University, 1968 (unpublished).
[13] H. S. Bennett, Bull. Am. Phys. Soc. 13, 1474 (1968).

TABLE VI. Comparisons of the longitudinal-optical phonon energy $\hbar\omega_l$ and the localized-oscillator energies $\hbar\omega_0$, $\hbar\omega_1$, $\hbar\omega_2$, and $\hbar\omega_3$. All the energies are expressed in terms of a.u.$\times 10^{-3}$ (10^{-3} a.u.$=0.0272$ eV$=4.133\times 10^{13}$ rad sec^{-1}).

	NaCl	KCl	MgO	CaO	SrO	CaF_2	SrF_2	BaF_2
$\hbar\omega_l$	1.18[a]	0.955[a]	4.80[a]	3.16[a]	1.95[a]	0.334[b]	0.271[b]	0.236[b]
$\hbar\omega_0(\alpha_0,\sigma_0)$	0.903	0.527	2.73	1.70	1.02	1.20	0.738	0.509
$\hbar\omega_2(\alpha_0,\sigma_2)$	0.909	0.542	2.64	1.68	1.03	1.28	0.779	0.542
$\hbar\omega_1(\beta_1,\sigma_1)$	0.914	0.554	2.58	1.68	1.03	1.30	0.775	0.550
$\hbar\omega_3(\beta_1,\sigma_3)$	0.892	0.525	2.69	1.70	1.04	1.23	0.748	0.525

[a] M. Born and K. Huang, *Dynamical Theory of Crystal Lattice* (Oxford University Press, Oxford, England, 1954), p. 85, Table 17.
[b] W. Kaiser *et al.*, Phys. Rev. **127**, 1950 (1962).

The SCP and HFPI models differ in many ways. One advantage which the HFPI models have over the SCP models is that no ambiguity exists in calculating the distant ionic polarization within the framework of the Franck-Condon principle. Because the SCP models allow the distant ions to violate partially the Franck-Condon principle, researchers must decide under what conditions and to what extent the distant ions may violate the Franck-Condon principle during an optical transition. This decision, which depends upon physical intuition, is the source of ambiguity and of differences among recent studies[14] and requires further study. The HFPI models have the advantage that they use less input data than the SCP models use but, at the same time, they require substantially more computer time than the SCP models require. A most important difference between the SCP models and the HFPI models is that the former predict spatially diffuse states for state C in NaCl and in KCl and for state B in CaF_2, SrF_2, and BaF_2, while the latter predict that all states are compact. This should be the case if the HFPI models are to be internally consistent with their assumptions. Observations, based on the predictions of the HFPI models and the SCP models (compare Table II of paper I and Tables II–V of the present paper), indicate that the spatial extent, the lifetime of state C, and the Huang-Rhys factor are closely interrelated. Keeping in mind that these models allow only radial changes in the F-electron wave function for state C, we note that Huang-Rhys factors greater than about 20 appear to be associated with at least one spatially diffuse state.

We see from Tables II and V that the HFPI (2) models for the F center in NaCl and in KCl agree well with the experimental absorption energies and with the fact that zero-phonon lines are not observed [S(abs)>6 and S(emis)>6], but disagree with the experimental emission energies and with the lifetimes of the relaxed excited states. We constrast this with the good agreement between the SCP model and experiment (Table II of paper I) for the above four quantities.

Both experimental and theoretical studies of the F center (one-defect electron) in the alkaline-earth oxides, particularly MgO and CaO and more recently SrO, contain many uncertainties. Tables III and V show that the HFPI (2) model for CaO predicts reasonable values for the absorption and emission energies, the zero-phonon transition energies, and the Huang-Rhys factors. We lack sufficient data on SrO to judge the agreement between the HFPI (2) model and experiment. At first sight, one may conclude that the HFPI (2) model fails to explain the F center in MgO, particularly, the large Huang-Rhys factor estimated by Henderson. Recent experimental studies[15] on MgO indicate that perhaps the F (one-defect electron) band and the F' (two-defect electrons) band lie sufficiently close to one another to obscure details of the spectra. This means that if the F band had zero-phonon structure on its tails ($S\lesssim 6$), it would be most difficult to observe due to the presence of the F' band. We might conclude then that the possibility of a Huang-Rhys factor less than 6 has not been excluded by present experiments. One unsolved mystery is why experiments on the F center in MgO seem to be qualitatively different from those in CaO. The F and F' bands in CaO are thought to be well separated. We compare this with what the HFPI (2) model seems to say. Except for the fact that the free-cation electronic polarizability of MgO is one-fifth that of CaO and one-ninth that of SrO, the input data in Table I is qualitatively the same for these three alkaline-earth oxides. Tables III and V reveal that the HFPI (2) models for MgO, CaO, and SrO predict qualitatively similar results. One might conclude from this that the ionic polarization is much more important in determining the optical properties of the F center in the alkaline-earth oxides than the electronic polarization is. We must wait for the completion of additional research before we might hope to resolve the above uncertainties.

It is most difficult to compare theory and experiment for the alkaline-earth fluorides because sufficient experimental data are not available. At present, we may only remark that the SCP(HF) model (Table III of paper I) gives much better agreement with the absorption experiments than the HFPI (2) model gives. Also, we observe that state B is diffuse for the SCP(HF) model and compact for the HFPI (2) model. Again, this dramatizes the need for further studies, both theoretical and experimental.

We conclude by comparing the present paper with Ref. 14. The researchers of both efforts examine the

[14] R. F. Wood (private communication); and R. F. Wood and U. Öpik, Phys. Rev. **179**, 783 (1969).

[15] J. E. Wertz (private communication).

behavior of the distant ions in some detail and must choose among various alternatives, none of which are completely satisfactory. The researchers of Ref. 14 study only the alkali halides and calculate the absorption and emission energies, some of the matrix elements which might appear in a lifetime calculation, the hyperfine interaction of the F electron with the nn ions in the ground state, and the relative positions of the $2s$- and $2p$-like levels which are important for the Stark effect. We do not calculate the latter two but instead calculate the zero-phonon transitions and the Huang-Rhys factors. They use a variational F-electron wave function which is orthogonal to the electronic orbitals of the neighboring ions. The orbitals are free-ion (unpolarized) Hartree-Fock orbitals. Both theories inlcude the classical ionic lattice to determine the relaxation of the nn in a breathing mode. They treat the ionic and electronic polarization in terms of the effective-mass approximation for the F center. We both rely upon the Franck-Condon principle to suggest the polarization during any optical transition. However, our respective methods differ substantially. They represent the ionic and electronic polarizations by a polarization potential written as the sum of the ionic polarization potential and the electronic polarization potential. These polarization potentials are not explicit functionals of the F-electron wave function and contain two additional parameters. Choosing reasonable values for these parameters is a troublesome process. The Franck-Condon principle and assumptions about the spatial extent of the F-electron wave function suggest various alternative procedures. One of the more successful ones states that the ionic polarization potential is zero for states A and B and that it contains for states C and D an effective dielectric constant determined by the effective-mass theory and the thermal ionization energy. On the other hand, our self-consistent polarization potentials for the HFPI models introduce no additional parameters into the theory and thereby do not require parameters whose values change when going from the absorption states to the emission states.

Both models attempt to satisfy the Franck-Condon principle during any optical transition. The ionic and electronic polarizations in the HFPI models respond for all states to the average F-electron charge density. The models of Ref. 14 allow the ionic polarization for the relaxed state C to follow to some extent the F electron. If the effective dielectric constant for the relaxed state C lies between the high-frequency dielectric constant and the static dielectric constant, then the ions must follow partially the F electron. But during an optical transition, the distant ions of both models do not follow the F electron because otherwise this would imply a change of the ionic polarization. Hence, the HFPI models compute state C in a different manner than do the Ref. 14 models. It is only when we treat the zero-phonon transition within the limitations of the Franck-Condon principle for the distant ions (classical) that the HFPI (2) model strains our physical intuition by allowing E(0-ph; abs,theory) to differ from E(0-ph; emis,theory). If the researchers of Ref. 14 had computed the zero-phonon transition, they would have encountered the same result. But this is of no quantitative consequence. The HFPI (2) model for the eight crystals studied here predicts quantitatively that the absorption and emission zero-phonon energies are essentially equal.

ACKNOWLEDGMENTS

The author is indebted to Dr. A. D. Franklin, Dr. B. Henderson, Dr. A. H. Kahn, and Dr. R. F. Wood for many informative discussions. He also thanks Dr. T. C. Ensign and Dr. H. J. Raveche for reading the manuscript.

APPENDIX A: POLARIZABLE LATTICE

Both of our polarizable-ion models require a study of the polarization about the defect. Polarizable-ion models contain an explicit evaluation of the polarization energy, while semicontinuum models relate the polarization energy to the Mott-Littleton radius. The change in electrostatic energy

$$W=\delta U=\delta(8\pi)^{-1}\int \mathbf{E}\cdot\mathbf{D}d^3r, \tag{A1}$$

which occurs when a point charge $-Z_v$ moves to the surface of the crystal is expressed in the semicontinuum models by the relation

$$W=-Z_v^2(1-\epsilon^{-1})(2R)^{-1}, \tag{A2}$$

where R is the Mott-Littleton radius, and ϵ is the appropriate dielectric constant. The electric field is $\mathbf{E}$, and the displacement vector $\mathbf{D}=\mathbf{E}+4\pi\mathbf{P}$, where $\mathbf{P}$ is the polarization vector (dipole moment per unit volume).

The author has previously discussed the ionic and electronic polarizations which a charge density $\rho_d(\mathbf{r})$ induces in an ionic crystal.[16] We therefore shall apply those results to the F-center problem. We consider an ionic crystal which contains one molecule $M_{n_+}X_{n_-}$ per volume v_c of the crystal. The volume of the unit cell is $v_c=\frac{1}{4}a^3$ and the lattice constant a is the cation-cation distance. The nn distance (cation-anion) is $r_1=\frac{1}{2}a$ for NaCl structures and $r_1=\frac{1}{4}\sqrt{3}a$ for CaF_2 structures.

We view the anions (e.g., $X=$O) and the cations (e.g., $M=$Ca) as polarizable point charges occupying the lattice sites. The anion ionicity is Z_- and the cation ionicity is Z_+. The unit cell is electrically neutral, $n_+Z_++n_-Z_-=0$. We also associate an ionic polarizability α_-^d or α_+^d and an electronic polarizability α_-^e or α_+^e with each ion in the lattice. These polarizabilities determine the response of the crystal to weak-static and high-frequency electric fields, respectively. In general, the polarizability is a tensor. However, we assume here for convenience that it is diagonal. This is a very reason-

[16] H. S. Bennett, J. Res. Nat. Bur. Std. **72A**, 475 (1968).

able assumption for cubic crystals such as CaO and CaF_2.

We compute the ionic polarizability from the repulsive interaction energy between the ionic cores E_r. When the νth ion moves a distance $|\mathbf{r}_\nu|\sigma_\nu$ towards one of its neighbors, it experiences a restoring force $\mathbf{F}_\nu$ due to the repulsive interaction E_r, i.e., $\mathbf{F}_\nu=-p_\nu\mathbf{r}_\nu\sigma_\nu$. The position of the νth ion in the perfect lattice is $\mathbf{r}_\nu$ and σ_ν is a dimensionless quantity which represents the distortion. The force constant p_ν is a linear combination of first- and second-order derivatives of the repulsive interaction E_r evaluated at $\sigma_\nu=0$. When we neglect the electronic deformation due to ionic motion and assume that the crystal is isotropic, the displacement (ionic) polarizability of the νth ion assumes the form

$$\alpha_\nu{}^d=(Z_\nu{}^2/p_\nu). \tag{A3}$$

We determine for both model HFPI (1) and model HFPI (2) the ionic polarization of the first shell of ions explicitly, and we determine the ionic polarization for all the remaining shells of ions from Eq. (A3). The ionic moment $[Z_\nu r_1\sigma/(1-\sigma)]\hat{r}_\nu$ for the νth ion on the first shell ($s=1$) represents the ionic polarization and is that moment which minimizes for a given F-electron state the total F-center energy. We obtain the electronic polarizabilities from Ref. 17.

We therefore represent an ion which is located at the lattice site $\mathbf{r}_\nu$ and which experiences a static electric field $\mathbf{E}(\mathbf{r}_\nu)$ as a point charge Z_ν located at $\mathbf{r}_\nu$ and upon which we superpose a point dipole moment

$$\boldsymbol{\mu}(\mathbf{r}_\nu)=(\alpha_\nu{}^e+\alpha_\nu{}^d)\mathbf{E}(\mathbf{r}_\nu). \tag{A4}$$

When the period of the electric field is much shorter than the characteristic period for ionic motion, but also longer than the orbital period for the electrons about the ion, the point dipole moment is $\boldsymbol{\mu}(\mathbf{r}_\nu)=\alpha_\nu{}^e\mathbf{E}(\mathbf{r}_\nu)$. When we view an ionic crystal as a dielectric continuum, the static dielectric constant ϵ_0 and the high-frequency (optical) dielectric constant ϵ_∞ give us information about the ionic and electronic dipoles which are induced by weak electric fields.

In order to make the present computations feasible, we shall consider only the spherically symmetric part $\rho(r)$ of the F-center charge density $\rho_d(\mathbf{r})$, i.e., we average $\rho_d(\mathbf{r})$ over the unit sphere

$$\rho(r)=(4\pi)^{-1}\int_0^{2\pi}d\phi\int_{-\pi}^{\pi}\sin\theta\,d\theta\,\rho_d(\mathbf{r}), \tag{A5}$$

where $r=|\mathbf{r}|$. The electric field $E_d(\mathbf{r})\hat{r}$ at the point $\mathbf{r}$ due to the defect charge density $\rho(r)$ is

$$E_d(\mathbf{r})=r^{-2}\int_0^r\rho(t)t^2dt. \tag{A6}$$

We then define the average defect charge $Q(r)$ contained within a sphere of radius r centered about $\mathbf{r}=\mathbf{0}$, namely,

$$Q(r)=\int_0^r\rho(t)t^2dt. \tag{A7}$$

We also define the average F-electron charge $Q_F(r;\eta)$ contained within a sphere of radius r by the relation

$$Q_F(r;\eta)=(4\pi)^{-1}\int_0^r t^2dt\int_0^{2\pi}d\phi\int_{-\pi}^{+\pi}\sin\theta\,d\theta \times\psi_\eta{}^*(\mathbf{t})\psi_\eta(\mathbf{t}), \tag{A8}$$

where $\psi_\eta(\mathbf{r})$ is the F-electron wave function.

The total electric field which the polarizable ion at $\mathbf{r}_\nu$ experiences is the sum of the electric field due to the defect charge density $\mathbf{E}_d(\mathbf{r}_\nu)$ and the electric field due to the dipoles induced on all the other ions except the ion at $\mathbf{r}_\nu$,

$$\mathbf{E}_{\rm tot}(\mathbf{r}_\nu)=\mathbf{E}_d(\mathbf{r}_\nu)+\sum_{\nu\neq\nu_1}{}'\,\mathbf{E}_{\rm dipole}(\mathbf{r}_\nu;\mathbf{r}_{\nu_1}). \tag{A9}$$

The Mott-Littleton procedure is an approximation which attempts to overcome the formidable task of solving the system of equations given by Eq. (A9). Following the first-order Mott-Littleton procedure,[18] we divide the crystal into two regions. Region I contains all the ions on shells centered about the F center and having a radius less than or equal to r_s. The radius r_s is the radius of the sth shell of ions centered about the F center. Region II contains all the remaining ions. The first-order Mott-Littleton procedure states that region I contains only the first ($s=1$) shell and that region II contains all the remaining shells.

We first outline the prescription for the dipole moments in region II. We view region II as a dielectric continuum. The electric field $\mathbf{E}$ and the displacement vector $\mathbf{D}$ are related in region II by the constitutive equation for a dielectric continuum.

$$\mathbf{D}=\mathbf{E}+4\pi\mathbf{P}=\epsilon\mathbf{E}, \tag{A10}$$

where ϵ is the appropriate dielectric constant and the polarization $\mathbf{P}$ is the dipole moment per unit volume,

$$\mathbf{P}(\mathbf{r})=\{(\epsilon-1)/4\pi\}\mathbf{E}(\mathbf{r}). \tag{A11}$$

The dipole moment per unit cell at $\mathbf{r}_l$ is $P_c(\mathbf{r}_l)=v_cP(\mathbf{r}_l)$. The Mott-Littleton prescription asserts that all dipole moments point in a radial direction from the defect and divides the dipole moment per unit cell among the (n_++n_-) ions contained in the unit cell in proportion to their individual polarizabilities,

$$\boldsymbol{\mu}_{\rm II}(\mathbf{r}_\nu)=\frac{\alpha_\nu}{(n_+\alpha_++n_-\alpha_-)}\frac{v_c(\epsilon-1)}{4\pi\epsilon_1}\mathbf{E}(\mathbf{r}_l)\hat{r}_\nu. \tag{A12}$$

[17] J. R. Tessman *et al.*, Phys. Rev. **92**, 890 (1953).

[18] N. F. Mott and M. J. Littleton, Trans. Faraday Soc. **34**, 485 (1938).

When studying the F center, one must distinguish between the electronic polarizations and the ionic polarizations. The electronic polarizations respond to rapid changes in $\rho_d(\mathbf{r})$ which occur whenever the F electron undergoes a transition from one state and another state. However, the ionic polarizations may not respond to such rapid changes in $\rho_d(\mathbf{r})$. Hence, when $\epsilon_1=\epsilon_\infty$, then ϵ must be ϵ_∞. When only electronic polarizations occur $\alpha_\nu=\alpha_\nu{}^e$, and when both electronic and ionic polarizations occur $\alpha_\nu=\alpha_\nu{}^e+\alpha_\nu{}^d$. Referring to Eq. (A12), we define the polarizability of an ion in region II by the quantity

$$M_{\mathrm{II}}(\nu)=\frac{\alpha_\nu v_c(\epsilon-1)}{4\pi\epsilon_1(n_+\alpha_++n_-\alpha_-)}. \tag{A13}$$

We introduce for convencince in discussing the region II the following notation:

$$M_\pm(\infty\,;e)=\frac{\alpha_\pm{}^e v_c(\epsilon_\infty-1)}{4\pi\epsilon_\infty(n_+\alpha_+{}^e+n_-\alpha_-{}^e)},$$

$$M_\pm(0;e)=\frac{\alpha_\pm{}^e v_c(\epsilon_0-1)}{4\pi\epsilon_0(n_+\alpha_+{}^T+n_-\alpha_-{}^T)},$$

$$M_\pm(0;T)=\frac{\alpha_\pm{}^T v_c(\epsilon_0-1)}{4\pi\epsilon_0(n_+\alpha_+{}^T+n_-\alpha_-{}^T)},$$

and

$$M_\pm(0;i)=M_\pm(0;T)-M_\pm(0;e),$$

where $\alpha_\nu{}^T=\alpha_\nu{}^e+\alpha_\nu{}^d$.

The radial component of the electric field at a site $\mathbf{r}_1$ in region I due to all the dipole moments in region II may be written in the form[16]

$$E_{\mathrm{out}}(\mathbf{r}_1)=r_0{}^{-5}\sum_{s\geq 2}Q(r_s)M_{\mathrm{II}}(s)D(s;\mathbf{r}_1), \tag{A14}$$

where $|\mathbf{r}_1|=r_0$ is the nn distance in the perfect lattice. Each shell s of ions has the same type of ions, and each ion of shell s exhibits the same polarizability $M_{\mathrm{II}}(s)=M_{\mathrm{II}}(\nu)$. The dipole coefficients $D(s,\mathbf{r}_1)$ for each shell are tabulated in Ref. 16 for values of $s\leq 21$. We also define the following partial sums over cations only and over anions only:

$$F_{+(-)}(\eta)=\sum_{\substack{s\geq 2\ \text{cations}\\ (\text{anions})\ \text{only}}}Q(r_s)D(s;r_1),$$

$$a=\sum_{\substack{s\geq 2\\ \text{cations only}}}D(s;r_1),$$

and

$$b=\sum_{\substack{s\geq 2\\ \text{anions only}}}D(s;r_1).$$

The first shell about an anion defect contains n_+ cations at a distance $r_1=r_0$ from the F center. Again, we assume that the induced dipole moment on an ion in the first shell points in a radial direction and has a magnitude μ_1. The radial electric field at the site $\mathbf{r}_1$ due to the dipole moments $\mu_1\hat{r}_\nu$ of the (n_+-1) other ions on the first shell is

$$E_1\hat{r}_1=r_1{}^{-3}\mu_1C_1\hat{r}_1, \tag{A15}$$

where the same shell dipole coefficient C_1 is a constant for a given lattice structure. The system of equations represented by Eq. (A9) reduces in the first-order Mott-Littleton approximation to one equation for the one unknown dipole moment $\mu_1\hat{r}_1$, namely,

$$\mu_1\hat{r}_1=\alpha[\{r_1{}^{-2}Q(r_1)+E_{\mathrm{out}}(r_1)\}/\{1-r_1{}^{-3}\alpha_1C_1\}]\hat{r}_1. \tag{A16}$$

The potential at the point $\mathbf{r}$ due to all the dipoles $\boldsymbol{\mu}(\nu)$ at $\mathbf{r}_\nu$ is

$$\phi(\mathbf{r})=\sum_\nu \boldsymbol{\mu}(\nu)\cdot\mathbf{r}'(\nu)/|\mathbf{r}'(\nu)|^3, \tag{A17}$$

where $\mathbf{r}'(\nu)=\mathbf{r}-\mathbf{r}_\nu$. Noting the identity

$$\mathbf{r}'(\nu)/|\mathbf{r}'(\nu)|^3=\nabla_\nu|\mathbf{r}'(\nu)|^{-1},$$

where

$$\nabla_\nu=\hat{x}(\partial/\partial r_{\nu x})+\hat{y}(\partial/\partial r_{\nu y})+\hat{z}(\partial/\partial r_{\nu z}),$$

we have

$$\phi(\mathbf{r})=\sum_\nu \boldsymbol{\mu}(\nu)\cdot\nabla_\nu|\mathbf{r}'(\nu)|^{-1}. \tag{A18}$$

We introduce for use in Sec. III the quantities

$$A_\nu(\eta)=\{\mathbf{r}_\nu/|\mathbf{r}_\nu|^3\}\cdot\nabla_\nu\int d^3r\,|\mathbf{r}'(\nu)|^{-1}|\psi_\eta(\mathbf{r})|^2, \tag{A19}$$

and

$$B_\nu(\eta;\zeta)=\left\{\nabla_\nu\int d^3r\,|\mathbf{r}'(\nu)|^{-1}|\psi_\eta(\mathbf{r})|^2\right\}\cdot\left\{\nabla_\nu\int d^3r\,|\mathbf{r}'(\nu)|^{-1}|\psi_\zeta(\mathbf{r})|^2\right\}. \tag{A20}$$

The integrals which appear in Eqs. (A19) and (A20) have been evaluated for the hydrogenic wave functions.[19] Because the trial wave functions (5) and (6) are linear combinations of hydrogenic wave functions, we use the evaluations tabulated in Ref. 19 to compute the electronic and ionic polarizations of the HFPI (2) model.

The two models, HFPI (1) and HFPI (2), differ in the way we treat the polarization potential as given by Eq. (A18). We use in the HFPI (1) model only the spherically symmetric part of the polarization potential which arises from the dipoles induced on the ions. We consider rigorously in the HFPI (2) model the polarization potential which arises from the dipoles induced on the first two shells ($s=1$ and $s=2$) and consider only the spherically symmetric part of the polarization

[19] C. A. Coulson, Proc. Cambridge Phil. Soc. 38, 210 (1942).

potential which arises from all the other dipoles on shells $s \geqslant 3$. We illustrate this difference by writing the potential $\phi(\mathbf{r})$ in terms of summations over shells. We define the polarization potential operator which arises from the νth dipole $\phi_\nu(\mathbf{r})$, namely,

$$\phi_\nu(\mathbf{r}) = \mathfrak{y}(\nu) \cdot \nabla_\nu |\mathbf{r} - \mathbf{r}_\nu|^{-1}.$$

We write

$$\phi(\mathbf{r}) = \phi_<(\mathbf{r}; n) + \phi_>(\mathbf{r}; n),$$

where

$$\phi_<(\mathbf{r}; n) = \sum_{s=1}^{n} \sum_{\nu \in s} \phi_\nu(\mathbf{r}),$$

and

$$\phi_>(\mathbf{r}; n) = \sum_{s=n+1}^{\infty} \sum_{\nu \in s} \phi_\nu(\mathbf{r}).$$

The prescription for the model HFPI (1) is to approximate $\phi(\mathbf{r})$ by the expression

$$\phi(\mathbf{r}) \approx \phi_{>,\mathrm{sph}}(\mathbf{r}; 0).$$

The prescription for the model HFPI (2) is to approximate $\phi(\mathbf{r})$ by the expression

$$\phi(\mathbf{r}) \approx \phi_<(\mathbf{r}; 2) + \phi_{>,\mathrm{sph}}(\mathbf{r}; 2),$$

where $\phi_{>,\mathrm{sph}}(r; n)$ is the spherically symmetric part of $\phi_>(r; n)$.

Using only the spherically symmetric part of the polarization potential is equivalent to treating the polarized medium as composed of dipole shells centered about the anion vacancy. The effective charge $Q(r_s)$ induces a dipole moment $\{M_{\mathrm{II}}(\nu) S_s Q(r_s)/r_s^2\}\hat{r}_\nu$ on the sth shell and the spherically symmetric part of the polarization potential due to this dipolar shell is

$$\begin{aligned} \phi_{\mathrm{dip}}(s) &= -\{M_{\mathrm{II}}(\nu) S_s Q(r_s)/r_s^4\}, & r \leq r_s \\ &= 0, & r > r_s. \end{aligned} \quad \text{(A21)}$$

We shall list here the additional notation which we have used in Sec. III. The spherically symmetric part of the potential which arises from the polarizations induced by the effective vacancy charge Z_v [Eq. (4)] becomes

$$\phi_v(r) = -P(s; M_\nu(0; T); Z_v) \quad \text{for} \quad r_s < r < r_{s+1},$$

where when $s = 0$,

$$\begin{aligned} &P(0; M_\nu(0; T); Z_v) \\ &= Z_v \{ \sum_{t \geqslant 2} r_t^{-4} M_t(0; T) S_t + r_1^{-4} S_1 \alpha_+^e [1 - r_1^{-3} C_1 \alpha_+^e]^{-1} \\ &\quad \times [1 - r_1^{-3}(a M_+(0,T) + b M_-(0,T))] \} \end{aligned} \quad \text{(A22)}$$

for $0 < r < r_1'$, and when $s \geqslant 1$,

$$P(s; M_\nu(0,T); Z_v) = Z_v \sum_{t \geqslant s+1} r_t^{-4} M_t(0; T) S_t$$

for $r_s < r < r_{s+1}$. The quantity S_s is the number of ions on shell s, and r_s is the radius of the sth shell. Similarly, the spherically symmetric part of the potential which arises from the polarizations induced by the F-electron charge density $\rho_F(\mathbf{r}; \eta)$ [Eq. (3)] is

$$\phi_F(r) = -Z_F P(s; M_\nu(0; e); Q_F(\cdots, \eta)) \quad \text{for } r_s < r < r_{s+1},$$

where when $s = 0$,

$$\begin{aligned} &P(0; M_\nu(0; e); Q_F(\cdots; \eta)) \\ &= \sum_{t \geqslant 2} r_t^{-4} M_t(0; e) Q_F(r_t; \eta) S_t \\ &\quad + r_1^{-4} S_1 \alpha_+^e (1 - r_1^{-3} C_1 \alpha_+^e)^{-1} \{ Q_F(r; \eta) \\ &\quad - r_1^{-3} [M_+(0; T) F_+(\eta) + M_-(0; T) F_-(\eta)] \} \end{aligned} \quad \text{(A23)}$$

for $0 < r < r_1'$, and when $s \geqslant 1$,

$$\begin{aligned} P(s; M_\nu(0; e); Q_F(\cdots; \eta)) &= \sum_{t \geqslant s+1} r_t^{-4} M_t(0; e) \\ &\quad \times Q_F(r_t; \eta) S_t \end{aligned}$$

for $r_s < r < r_{s+1}$. We observe from Eqs. (A22) and (A23) that the first-order Mott-Littleton procedure gives the electronic polarizability of the ions on the first shell (region I) which arises from the effective vacancy charge Z_v in the form

$$\begin{aligned} \alpha_1^e(Z_v) &= \alpha_+^e (1 - r_1^{-3} C_1 \alpha_+^e)^{-1} \\ &\quad \times \{1 - r_1^{-3} [a M_+(0; T) + b M_-(0; T)]\} \end{aligned} \quad \text{(A24)}$$

and that it gives the electronic polarizability which arises from the angular average of the F-electron charge density $Z_F Q_F(r; \eta)$ in the form

$$\begin{aligned} \alpha_1^e(Q_F(\cdots; \eta)) &= \alpha_+^e [1 - r_1^{-3} C_1 \alpha_+^e]^{-1} [Q_F(r_1; \eta) \\ &\quad - r_1^{-3}(M_+(0,T) F_{F,+}(\eta) + M_-(0,T) F_{F,-}(\eta))], \end{aligned}$$

where (A25)

$$F_{F,+(-)}(\eta) = \sum_{\substack{s \geqslant 2 \text{ cations} \\ \text{(anions) only}}} Q_F(r_s; \eta) D(s; r_1).$$

When we allow the nn ions to move, we are in fact explicitly computing the ionic polarization of the first shell. Because the core electrons on the ions of shell $s = 1$ can respond to rapid changes in the total electric field which they experience, we use the total polarizability of the ions in region II, $M_\pm(0; T)$, in Eqs. (A24) and (A25).

APPENDIX B: TRANSITION MATRIX ELEMENTS

In order to compute the Haung-Rhys factors, we must compute the dipole transition matrix elements

$$T_{f,i}(T) = {}_T\langle n_f, \eta_f; \zeta_i, \sigma_f | z | n_i, \eta_i; \zeta_i, \sigma_i \rangle_T, \quad \text{(B1)}$$

where the total initial state is given by

$$|n_i, \eta_i; \zeta_i, \sigma_i\rangle_T = |\eta_i; \zeta_i, \sigma\rangle_F |n_i; \eta_i\rangle_L.$$

Because the distant ionic polarization always obeys the

Franck-Condon principle in the idealized model of Sec. VI, it does not change during an optical transition, and we have $\zeta_f=\zeta_i$. The dipole transition matrix element becomes

$$T_{f,i}(T)=T_{f,i}(F)T_{f,i}(L)={}_F\langle\eta_f;\zeta_i,\sigma_F|z|\eta_i;\zeta_i,\sigma_i\rangle_F \times{}_L\langle n_f;\eta_f|n_i;\eta_i\rangle_L, \quad \text{(B2)}$$

where the lattice overlap integral

$$T_{f,i}(L)={}_L\langle n_f;\eta_f|n_i;\eta_i\rangle_L$$

is

$$T_{f,i}(L)=\prod_{\nu\in\Gamma_1}^{S_1}\int_{-\infty}^{+\infty}U_{\eta_f,n_f}(X_\nu)U_{\eta_i,n_i}(X_\nu)dX_\nu. \quad \text{(B3)}$$

We define

$$T_{f,i}(L,\nu)=\int_{-\infty}^{+\infty}U_{\eta_f,n_f}(X_\nu)U_{\eta_i,n_i}(X_\nu)dX_\nu. \quad \text{(B4)}$$

Using Eq. (54), we write

$$T_{f,i}(L,\nu)=N_{n_i}(\gamma_i)N_{n_f}(\gamma_f)\int_{-\infty}^{+\infty}H_{n_f}(\gamma_f y_f)e^{-\frac{1}{2}\gamma_f{}^2y_f{}^2} \times H_{n_i}(\gamma_i y_i)e^{-\frac{1}{2}\gamma_i{}^2y_i{}^2}dX, \quad \text{(B5)}$$

where $y_f=r_1(\sigma-\sigma_f)$, $y_i=r_1(\sigma-\sigma_i)$, and $dX_1=r_1d\sigma$. Introducing the notation $\gamma=\gamma_i/\gamma_f$, $z=\gamma_f r_1(\sigma_i-\sigma_f)$, and $y=\gamma_f y_f$, we have $\gamma_i y_i=\gamma(y-z)$, and we obtain

$$T_{f,i}(L,\nu)=\gamma_f{}^{-1}N_{n_f,n_i}\int_{-\infty}^{+\infty}H_{n_f}(y)e^{-\frac{1}{2}y^2} \times H_{n_i}(\gamma(y-z))e^{-\frac{1}{2}\gamma^2(y-z)^2}dy, \quad \text{(B6)}$$

where $N_{n_f,n_i}=N_{n_i}(\gamma_i)N_{n_f}(\gamma_f)$. We then complete the square of the exponent and use the notation

$$\xi=\{\tfrac{1}{2}(1+\gamma^2)\}^{1/2}(y-y_0), \quad y_0=\gamma^2z(1+\gamma^2)^{-1}=\delta\xi_0,$$
$$\delta=\{\tfrac{1}{2}(1+\gamma^2)\}^{-1/2}, \quad \xi_0=\gamma^2z\{2(1+\gamma^2)\}^{-1/2},$$

and $y=\delta(\xi+\xi_0)$. We find that the lattice-overlap integral for the νth ion becomes

$$T_{f,i}(L,\nu)=\gamma_f{}^{-1}N_{n_f,n_i}\delta e^{-\gamma^2z^2/2(1+\gamma^2)}\int_{-\infty}^{+\infty}d\xi\, e^{-\xi^2} \times H_{n_f}(\delta(\xi+\xi_0))H_{n_i}(\gamma\{\delta(\xi+\xi_0)+z\}). \quad \text{(B7)}$$

We are interested in the case for which $n_i=0$. Referring to Ref. 20, we reduce Eq. (B7) to the expression

$$T_{f,i}(L,\nu;n_i=0)=\pi^{1/2}\gamma_f{}^{-1}N_{n_f,0}\delta e^{-\gamma^2z^2/2(1+\gamma^2)} \times\sum_{m=0}^{m\le n_f/2}\frac{(2\delta\xi_0)^{n_f-2m}n_f!}{(n_f-2m)!}\sum_{l=m}^{2m}\frac{(\delta-1)^l2^{2m-l}}{(2m-l)!(l-m)!}, \quad \text{(B8)}$$

where $\pi^{1/2}N_{n_f,0}\gamma_f{}^{-1}=(\gamma/2^{n_f}n_f!)^{1/2}$. When $n_f=0$, we have

$$T_{f,i}(L,\nu;n_i=0,n_f=0)=\gamma\delta e^{-\gamma^2z^2/2(1+\gamma^2)}. \quad \text{(B9)}$$

The square of the matrix element gives us the transition probability. The transition probability for a zero-phonon transition from state A to state H or from state C to state G is proportional to $|T_{f,i}(L;n_i=0,n_f=0)|^2$, namely,

$$T_{0-\mathrm{ph}}\propto(\gamma\delta)^{2S_1}e^{-S_1\gamma^2z^2/(1+\gamma^2)}. \quad \text{(B10)}$$

We obtain from Eq. (B7) or from Eq. (B10) the Huang-Rhys factor

$$S=\frac{S_1\gamma_i{}^2r_1{}^2(\sigma_i-\sigma_f)^2}{1+(\gamma_i/\gamma_f)^2}. \quad \text{(B11)}$$

[20] P. M. Morse and H. Feshbach, *Methods of Theoretical Physics* (McGraw-Hill Book Co., New York, 1953), Part I, pp. 786–787.